Real-time multi-objective optimisation for electric vehicle charging management

Ridoy Das[a], Yue Wang[b1], Krishna Busawon[c], Ghanim Putrus[c], Myriam Neaimeh[a]

[a] Newcastle University, Power Systems Research Group, Newcastle upon Tyne, NE1 7RU, United Kingdom.

[b] University of Chichester, Department of Engineering and Design, Upper Bognor Rd, PO21 1HR, Bognor Regis, United Kingdom.

[c] Northumbria University, Electrical Power and Control System Research Group, 2 Ellison Place NE1 8ST, Newcastle upon Tyne, United Kingdom.

Nomenclature

Acronyms	
AHP	Analytical Hierarchy Process
ANEC	Augmented Non-dominated ε-constraint algorithm
ANN	Artificial neural network
DN	Distribution network
DP	Dynamic programming
DS	Distribution system
DSO	Distribution system operator
EV	Electric vehicle
GB	Great Britain
GUI	Graphical user interface
HMG	Home-micro-grid
LP	Linear programming
MG	Micro-grid
MOO	Multi-objective optimisation
MPC	Model-predictive control
OMODP	Online multi-objective dynamic programming
PV	Photovoltaic
RES	Renewable energy sources
SOC	State of Charge
UK	United Kingdom
Sets and Indices	
t	Current simulation time step
t^m	Measurement time step
m	Maximum number of objective functions
n	Dimension of the decision space
q	Maximum number of discrete SOC values
i,j	Indices of discrete SOCs
k,l	Indices of objective functions
Δt	Time interval, 15 min
N^s	Total number of time steps
S^q	Set of discrete SOC values
W_t^1, W_t^2	Set of discrete SOC values satisfying power limit and energy requirement constraints
X_t^q	Feasible set of discrete SOCs at time t
$\boldsymbol{X}$	Generic feasibility set
S_t^{op}	Optimal SOC chosen at time t

[1] Corresponding author: yue.wang@chi.ac.uk, University of Chichester, Engineering and Design, Bognor Regis.

$\mathbf{P}_t^q$	Pareto frontier at time t
σ_t	Set of optimal SOCs with MPC
σ_t^q	Set of discrete counterparts of the SOCs determined with MPC
χ_t^q	Set of feasible discrete SOC states with DP formulation and MPC

Constants

C^B	Battery investment cost (£/kWh)
$\bar{E}^{EV}$	EV battery capacity (kWh)
$\underline{E}^{EV}$	Minimum EV energy limit (kWh)
$\bar{P}^{EV}$	Charging/discharging rating of the charger (kW)
η^+, η^-	Charging and discharging efficiency of EV charger

Parameters

P_t^d	Household electricity demand at time t (kW)
P_t^{PV}	PV generation at time t (kW)
π_t	Real-time electricity price at time t (£/kWh)
DOD	Depth of discharge
$[\gamma_1, \dots, \gamma_8]$	Fitting parameters of the empirical battery degradation model
T^b	Battery temperature (°)
$\langle SOC \rangle$	Average SOC in N^s time steps
C_t^r	Charging/discharging rate at time t
E^{req}	Energy requested for next trip
t^{arr}	Arrival time step
t^{dep}	Time step for next departure
t^{meas}	Measurement time slot
SOC^{in}	SOC at the beginning of the simulation step
SOC^{arr}	SOC of the EV at arrival
SOC^{dep}	SOC of the EV at departure
S^A, S^B	Discrete counterparts of the arrival and departure SOCs
$[\beta^1, \dots, \beta^m]$	Priorities of the objectives indicated by the stakeholders
S_t^*	Globally optimal SOC from AHP at time t
P_t^{EV}	Power exchanged by the EV battery (charging or discharging)
$V_{t^{meas}}^b$	Voltage of the battery at time t^{meas}
$I_{t^{meas}}^b$	Current in/out of the battery at time t^{meas}
$SOC_{t^{meas}}$	SOC of the battery at time t^{meas}

Functions

I_t^{b*}	Current set point for the charger
$\mathcal{F}_1$	Energy cost of the HMG (£)
$\mathcal{F}_2$	Battery degradation cost (£)
$\mathcal{F}_3$	Net power exchanged between HMG and grid (kWh)
α_t^c	Cycling degradation coefficient
E_t^{EV}	Energy stored in the EV at time t (kWh)
$\mathcal{F}$	A generic objective function

Decision variables

P_t^{EV+}, P_t^{EV-}	Charging and discharging power of the EV (kW)
S_t^q	Discrete value of SOC at time t
$\mathbf{x}, \mathbf{x}'$	Generic decision variables

1

1   **Abstract**

2   The continuous increase in the uptake of electric vehicles and the interest to use electric

3   vehicles to provide energy services require commercially viable business models for all

4   involved stakeholders. It is, however, challenging to achieve the synergy among different

5   stakeholders since their objectives are often conflicting. This work proposes a real-time multi-

6   objective optimisation method where electric vehicle charging/discharging profile is scheduled

7   in real-time to strike a balance among different objectives, namely electricity cost reduction,

8   battery degradation minimisation and grid stress alleviation as well as meeting the electric

9   vehicle user charging requirement by fulfilling the departure time. Dynamic programming is

10   adopted due to its computational efficiency, which is suitable for real-time applications. The

11   effectiveness of the proposed method is demonstrated using a residential case study where the

12   house is equipped with an electric vehicle and a photovoltaic system, and is validated by

13   experimental implementation. The results show that the proposed multi-objective optimisation

14   algorithm achieves the set objectives to satisfy the stakeholders' priorities and provides a profit

15   for the electricity end-user that is double as compared to that achieved by a benchmark multi-

16   objective algorithm. The results demonstrate the effectiveness of the proposed multi-objective

17   method and its suitability for real-time charging/discharging scheduling.

18   **Keywords**

19   Multi-objective optimization, real-time optimization, V2G, electric vehicles, renewable
20   energy, decentralized control.

21   **Highlights**

22   -   Three objectives, energy cost, battery degradation and grid exchange are optimised.
23   -   Multi-objective real-time optimisation with dynamic programming is implemented.
24   -   The algorithm computes electric vehicle control set points within few seconds.
25   -   The algorithm optimised multiple objectives in an experimental demonstration

26   # 1. Introduction

27   The global energy landscape is going through a transformative phase where the increasing

28   penetration of renewable energy is phasing out conventional fossil fuel-based electricity

29   generation plants. An equally important phenomenon is electro-mobility, which is envisioned

30   by several countries as the definitive step to develop their transportation systems towards an

31   ecosystem with net-zero emissions. This is evidenced by the encouraging numbers on global

32   electric vehicle (EV) deployment, which stands at 7.2 million vehicles as of 2019 [1]. Forecasts

33   indicate that by 2030 there will be up to 250 million EVs on the roads [1]; 2.4-3.6 million in

the UK only [2]. With the increasing number of EVs usage, their energy requirement rises concurrently. Without any means of controlling their charging, EVs could increase the UK electricity system peak by 24 GW by 2050 [2]. In contrast, EVs provide a unique energy storage capability to support renewable energy generation and the electricity grid. In fact, EVs can be suitably controlled to support a rooftop photovoltaic (PV) system in order to provide the household electricity demand and reduce the electricity bill [3]. This is made possible by Vehicle-to-Grid (V2G) technology. However, questions still remain on the effectiveness of this technology, the profitability of V2G and the impact of this on battery degradation [4], [5], [6].

Published research have devoted considerable efforts in developing real-time optimisation models by considering the nature of the optimisation process, optimisation strategy, multi-objectivity, computational efficiency and experimental demonstration. The review of the current literature on real-time optimisation has been structured according to these features as the present work aims at developing a practicable optimisation method that can provide the best results in these categories. Table 1, provides a summary of the features of the reviewed literature.

1. Table 1 Summary of the main features of the optimisation methods for the reviewed literature

Literature	Type	Optimisation method	Multiple objective consideration	Time horizon	Computational time
[8]	Centralised	Heuristic	Two objectives combined	One minute	Few seconds
[9]	Decentralised	Scheduling algorithm and classical optimisation	Two objectives combined	No info	No info
[10]	Centralised	Meta-heuristic	Two objectives combined	Half-hour	44 s
[11]	Centralised	Meta-heuristic	Two objectives combined	One hour	66 s
[12]	Centralised	Two-stage stochastic program	Two objectives combined	One hour	No info
[13]	Mixed centralised and local decision	Convex optimisation	Two objectives sequentially optimised	One hour	No info
[14]	Centralised	Linear program	Single objective	15 minutes	Within one second
[15]	Decentralised	Classical optimisation	Two objectives	Two modes:	Within seconds

4

		and droop control		slow with 15 min time frame and fast with second based time frame	
[16]	Centralised	Meta-heuristic	Two objectives sequentially optimised	15 min	No info
[17]	Centralised	Combined heuristic and classical optimisation	Three objectives combined	5 min	No info
[18]	Two-layer, mixed centralised and decentralised	Meta-heuristic	Three objectives combined	One hour	No info
[19]	Decentralised	State-space based control	Two objectives combined	One hour	Within two minutes
[20]	Decentralised	Bayesian optimisation	Two objectives combined	15 minutes	8 minutes
[21]	Decentralised	Classical optimisation	Single objective	One hour	No info
[22]	Decentralised	Dynamic programming	Two objectives combined	No info	Within seconds

1   In the field of optimisation and control, the trade-off between centralised and decentralised

2   strategies must be considered when developing an energy management framework. This holds

3   true also for real-time optimisation methods. In fact, in centralised control algorithms, whereby

4   a central manager has an overarching view upon the system, allow a system-wide knowledge

5   and enable a comprehensive management capability of the controllable assets, leading to an

6   optimal operation [7]. This comes at a cost of higher computational burden and poor scalability

7   as any addition to the system implies an increase in complexity [7]-[16]. This approach was

8   widely adopted for problems related to optimal network management, [8], [9], [11], [12], [16],

9   [17], where a central third party issued optimal operation schedules in order to minimise

10   operational costs, increase RES utilisation or ensure an efficient operation of the grid. To offset

11   the computational complexity, the central decision step was often followed by a local

12   management stage (see eg. [10], [11], [12], [13], [15], [18]). On the other hand, decentralised

13   optimisation strategies aim to control assets in situ, with the aid of local measurements [7]. The

present work falls in this category. This class of strategies are implemented to pursue the interests of end-users, i.e. end-electricity consumer or EV user, and are suitable for large scale optimisation. It was demonstrated in [15], [19], [20], [21] and [22] that decentralised management can be exploited to control a large number of users, by minimising users' operational cost [20], [22] and improving the operation of distribution networks [15], [19], [21]. However, these models do not have global information, which may lead to sub-optimal solutions for a community of users. To this end, an aggregated control method where clusters of EV users were optimally scheduled with some coordination was developed in [19]. In [20], a Bayesian game approach where users could communicate with their neighbours and take optimal decisions even with imperfect operation was proposed.

Since there is a wide variety of systems that need to be optimised, with each one having different properties, the optimal control method needs to adapt to the characteristics of the system. To this end, a range of optimisation techniques are available in the literature; namely linear models [14] (when integer variables are used these become mixed integer linear program), convex optimisation, heuristic methods (see eg. [8] and [15]) and meta-heuristics methods [10], [11], [15], [18]. In particular, methods such as Grey Wolf algorithm, Genetic Algorithm, and Particle Swarm algorithm were applied in [10], [11], [15] and [18], due to the non-convexity feature of their models. Although with random initialisation of the search space and heuristic based iterative processes these algorithms avoid getting trapped in local optima, they necessitate substantial time for providing the charging schedule for one time step (the time required to compute the charging schedule for one time step is designated as computational time throughout this paper). In fact, with simulation time steps of half an hour, computational times of 44 and 66 seconds were reported in [10] and [11] respectively, as compared to [8], which algorithm responded within one second. Different from the other studies, a dynamic programming was implemented in [22] to obtain a global solution to the optimisation problem. Another aspect that needs to be addressed during optimisation is the consideration of uncertain variables, such as generation from RES and EV parking time. For this purpose, stochastic optimisation [11], [12], robust optimisation [20] and Monte Carlo simulation [9], [15] are notable methods. In contrast historical data to develop prediction models to inform the optimisation process were used in [10], [13], [16], [18], [21] and [22].

Electricity system operators, original equipment manufacturers (OEMs), service providers, i.e. electricity utility companies, charging operators, aggregators and crucially end-users are all involved in a symbiotic ecosystem that is based upon the partnership between the energy and

the transportation sectors. At the core of this promising endeavour, several objectives, albeit conflicting at times, must be achieved. These include cost minimisation [8]-[10], [12]-[14], [18], [20], [22], optimal operation of electricity distribution networks (DNs) [11] - [19], [21], i.e. improve voltage stability [23], reduce losses and balance the system, reducing charging time of EVs [8], [14], [17] and only in one case battery degradation minimisation [22]. Furthermore, most of the existing literature on real-time optimization does not investigate multi-objective properties in detail. Among these limited works, the majority considered two objectives such as [11], [12], [13], [17], [20], and only one suggested the trade-off between two objectives, [22],. In fact, when two or more objectives are conflicting, the trade-off between them must be highlighted. This is often done with a Pareto analysis, where the objective values resulting from the application of different decision variables to all the relevant objective functions are organised in a manifold, called Pareto frontier. This frontier shows the behaviour/tendency of the other objectives when one objective is optimised, and therefore highlights conflicts and agreements, i.e. when minimising one objective the others can also be minimised, remain unaffected, or in the worst case maximised. It is therefore crucial to perform a Pareto analysis when dealing with multiple conflicting objectives, as done in the present research. However, none of the literature investigating real-time optimisation performed Pareto analysis. In this paper, the Pareto analysis has been performed with an improved dynamic programming approach, which, due to the significantly lower computational time, is best suited for real-time applications.

Real-time control of EV charging also requires optimal and timely schedules to be communicated to EV chargers, which then execute the charging/discharging commands. This is a key requirement as charging commands need both to be accurate and fast considering that there is often a time-window which marks the deadline for decision-making. This unavoidably implies a trade-off between the above two requirements as rapid decisions may compromise optimality and endless computation entails missing the deadlines. Some research works have proposed fast methods [8], [15], that can respond in a matter of seconds, while some take up to eight minutes [20]. This is because, while a heuristic decision chart and droop control were proposed in [8] and [15], respectively, game-theoretical approach under incomplete information was presented in [20], which required the algorithm to converge to a stable solution. Since their underlying time steps were different – seconds in [8] and [15] and 15 minutes in [20] – both approaches complied with their time limits. As discussed above, in general, decentralised [19] and heuristic based [22] algorithms performed faster (one to few

seconds) than centralised and meta-heuristic methods [10], [11] (44 and 66 seconds respectively).

On the other hand, while several optimal charging scheduling methods can be found in literature [10]-[22], it turns out that only few have been experimentally demonstrated [8], [9], and none had multi-objective properties. This represents a fundamental gap as empirical tests accelerate the process of prototyping with the aim of a swift commercialisation. To this end, a cloud-based application with user-interface was developed in [8], where drivers could set future destinations and then an intelligent algorithm directed them to the best charging station that minimised charging cost and time. A priority-based charging scheme was tested by [9] on 15 EVs, and their method was able to incentivize drivers in order to consume more renewable. However, their approach required EV users to modify their travelling requirements to obtain a better priority, which would undermine the wide adoption of EVs. In fact, their proposed algorithm would not guarantee the satisfaction of all users, whereas, EV user's requirements should be given the highest priority, as implemented in the present work.

In [24], an augmented non-dominated ε-constraint (ANEC) algorithm was proposed to solve the multi-objective EV charging problem. Three objectives, namely, electricity cost, battery degradation cost and grid net exchange were optimised. The ANEC algorithm is compatible to problems with conflicting objectives and the trade-off among the three objectives was solved by analytical hierarchy process (AHP). However, as the method was developed for day-ahead implementation, a real-time optimisation framework and its implementation in an experimental setup was not investigated.

To summarise, there is a lack of decentralised, real-time, multi-objective EV scheduling model that is readily implementable on charging equipment and the present work aims to fill this gap in the area of optimal EV charging scheduling.

1.1. Main Contributions

The present research aims at optimising the charging and discharging process of EVs by integrating all the crucial techno-economic parameters in a real-time management system. Based on the reviewed literature a number of key research gaps have been identified and these are summarised in two main points as:

- There is a lack of a systematic approach in the area of real-time EV
  charging/discharging scheduling for optimising multiple objectives. Analysing the

trade-off between multiple conflicting objectives, given by the interests of different stakeholders, is essential, which has not been implemented in combination with real-time operation. This point is especially critical because all assets (non-controllable loads, controllable loads, renewable energy generation, stationary storage and EVs) connected to the distribution network will have consequences on all the involved stakeholders. Therefore, to ensure that low carbon technologies are widely adopted, the interests of all stakeholders must be taken into account. However, none of the reviewed research works considered this aspect.

- The majority of the proposed optimisation methods have been validated only through simulations. While some studies provided experimental demonstration, to the best knowledge of the authors, there has not been any experimental demonstration of multi-objective charge control of electric vehicles to date.

The contributions of the present work are as follow:

1) Implementation of real-time multi-objective optimisation of three key objectives, namely end-user electricity cost, battery degradation cost and grid net exchange, in line with the interests of the main smart grid stakeholders, which has not been proposed in literature thus far.
2) Solving a nonconvex problem with satisfactory computational efficiency by using dynamic programming, which demonstrates the suitability of the proposed method to real-time applications, is easily scalable and safeguards user privacy.
3) Experimental demonstration of the proposed method in a small-scale setup, with the aid of an intuitive graphical user interface (GUI).

The remainder of the paper is organised as follows: Section 2 formulates the real-time multi-objective optimisation problem for a household equipped with a PV system and an EV. Three objectives functions are defined based on economic and operational targets. A novel DP based MOO algorithm is presented in Section 3. In Section 0, the details of the seven case studies are provided, where the first four are simulation based and carried out in Section 5. Three additional experimental cases are presented in Section 6, where the algorithm is applied to a small-scale laboratory setup. Finally, Section 7 presents key conclusions and discusses the applicability of the proposed approach for future applications.

2. Problem formulation

In this section, a multi-objective optimisation framework is formulated. The aim is to control charging and discharging of the EV battery in a household micro-grid (HMG). The schematic of a prospective HMG is provided in Figure 1.
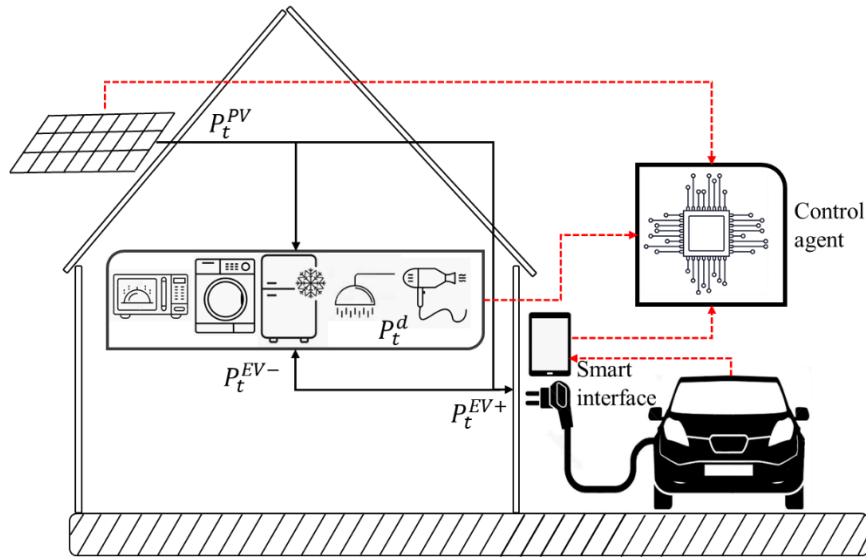

Figure 1. Schematic of an HMG with physical power exchange (black) and communication links (red dashed)

The HMG includes household appliances which demand electrical power and a photovoltaic (PV) system, which demands and generate electrical power, respectively. The aim is to optimise the power exchanged by the EV in order to fulfil a number of technical and economic objectives. An optimal control strategy for the charging/discharging process of the EV battery is implemented by developing an agent/controller that receives local measurements, and based on the status of the micro-grid, controls the charging/discharging of the available EV. Finally, it must be pointed out that the proposed method falls in the class of decentralised optimisation strategies, as each HMG in a DN/neighbourhood/street can implement this framework while coordinated by the system operator.

The main objective is to control the charging infrastructure; therefore, real-time or online control algorithms are essential. This approach differs from deterministic approaches, where all the information is known ahead to time. In this new context, only measurements of the status of the system are available and future status are unknown. Therefore, forecasts of system variables are required to estimate the future state of the system. In addition, decisions on the optimal scheduling will have to be implemented within a fixed period as the optimisation

1   window is discretised in fixed steps. A schematic of the scheduling flow is provided in Figure

2   2.
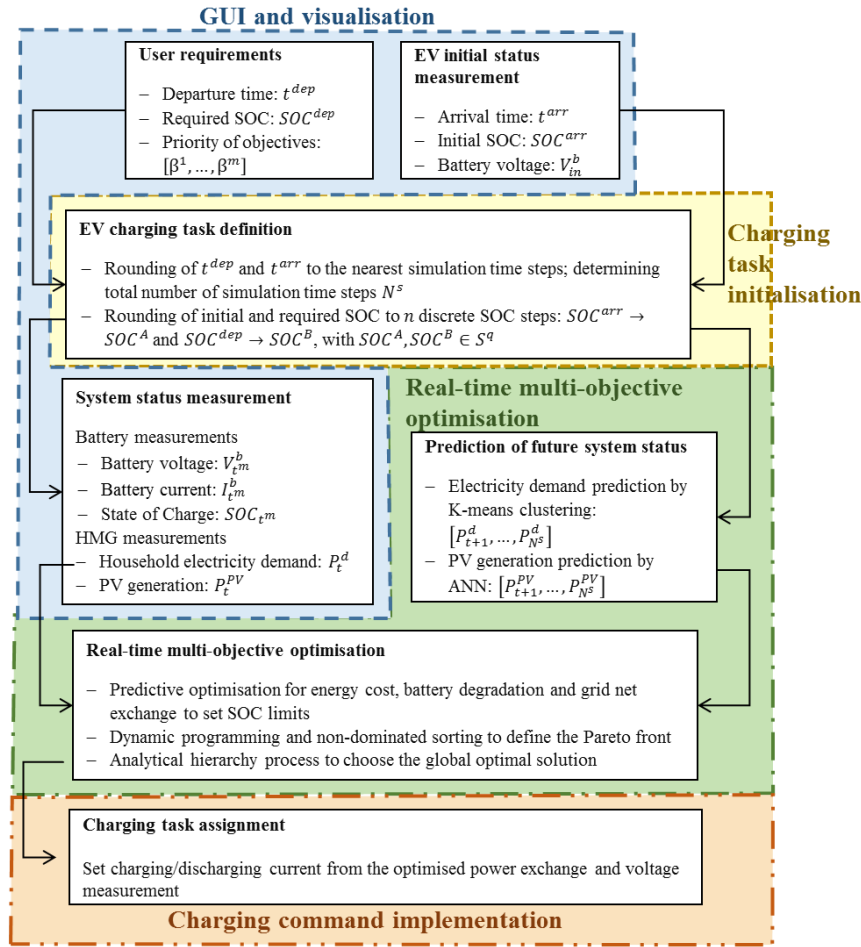
Figure 2. Flow diagram for real-time scheduling of an HMG

5   The system will initiate when an EV is connected to the HMG through the charger. The EV

6   will be considered available from the nearest approximated time step and the time will be

7   recorded. The real-time optimisation system is initiated by the user by giving its consensus to

8   operate the EV. This is aligned with the approaches available in real-life [25], where upon

9   arrival, the EV user plugs the car in the charger. Then, they communicate the time for the next

10   departure and the minimum level of energy they require. The EV user also specifies their

11   priorities for the three objectives; more details can be found in the next paragraphs. The user

12   submits the charging/discharging task and monitors the system status, i.e. battery and HMG

13   parameters through a GUI, which allows a simple interaction capability. Based on the demands

14   of the EV user a charging/discharging task is built and submitted to the system. The system is

15   then initialised by measuring its initial status, which is made by the following information:

16   -   Battery minimum voltage

1 - Battery maximum voltage

2 - Battery initial voltage

3 - Time at initiation

4 - Wholesale electricity price

5 The number of available time steps before departure and the associated state of charge (SOC)

6 variation limits are also calculated; this is done in the initialisation step; more details will be

7 provided in Section 3 where the algorithm is explained. Two functions constitute the real-time

8 multi-objective operation process, namely prediction and main optimisation. In this step, the

9 two main system variables, namely the household electricity demand and PV generation are

10 forecasted, using state-of-the-art techniques [10], [13], [16], [18], [21], [22]. Next, the main

11 optimisation process can be initiated and a charging/discharging command for the current time

12 step will be provided. Finally, in the charging implementation step, the charging/discharging

13 command is converted as a reference signal for the available charging facility which then

14 establishes the power/energy exchange. The system's status, i.e. the EV SOC is updated (since

15 a charging or discharging process is carried out) and this is recorded with the measurement

16 system. Voltage, current, power and energy exchanged with the battery are constantly

17 monitored throughout the whole task, and data is continuously logged to inform the

18 optimisation process, in order to update and better regulate the charging/discharging policy;

19 this information is constantly updated in the GUI. Once the charging deadline has been reached,

20 the system goes in standby.

21 2.1. Mathematical model

22 In this section, the main algorithm for implementing real-time multi-objective optimal

23 scheduling of EV charging/discharging will be discussed. The proposed algorithm improves

24 the ANEC method proposed in [24] for real-time implementation. In Section 5, a comparison

25 between the proposed real-time optimisation method and ANEC is presented.

26 The aim of this research is to develop a rational agent which manages the energy exchange in

27 the HMG by controlling the energy exchanged by the EV. A number of assumptions are

28 required for developing a coherent mathematical model that best fits the physical system, and

29 these are listed hereby.

30 – EV driving requirements are taken as constraints, and plug-in and plug-off times are

31 approximated to the nearest quarter of an hour.

- We assume a variable electricity price which replicates the electricity wholesale market price with distribution and transmission charges. As the wholesale price is known one day ahead, this does not bring uncertainty to the model. An aggregator will ensure these contractual terms are complied.

- EV chargers can regulate the output power continuously. This is in line with the experiments performed in this work.

- Battery charging and discharging processes cause the same battery degradation, which is aligned with the findings from [29].

- A dataset of historical electricity demand profiles is available each HMG. This is reasonable as smart meters are rolled out and will be used in the future for smart grid applications, as the one proposed in this paper.

While pursuing the most beneficial policy for the owner, the agent will need to ensure key objectives that are important for the involved stakeholders. This is because, as discussed in [24], if the interest of only one stakeholder is considered, then the society will achieve only a sub-optimal operation. Whereas, if the whole set of options are made available to the user and the trade-off between the different objectives are explicated, then the user (or the agent which acts on their behalf) can make an informed decision that can benefit all the involved stakeholders. As proposed in [24], the main stakeholders considered in this work are:

1) The end-electricity user, who wants to minimise the energy cost of the HMG (Obj_1).

2) The EV user, who wants to preserve the life of the EV; hence, minimise battery degradation (Obj_2,).

3) Distribution system operator (DSO), who wants to alleviate potential grid stress (Obj_3,).

2.1.1. Optimisation objectives

Hereafter, the objectives associated with the three key stakeholders are mathematically modelled.

End-user electricity cost

The energy cost incurred by the HMG owner for N^s time steps can be formulated as below.

$$\underset{P_t^{EV+}, P_t^{EV-}}{argmin} \ \mathcal{F}_1 = \sum_{t=1}^{N^S} \left[\left(P_t^d - P_t^{PV} + P_t^{EV+} - P_t^{EV-} \right) \Delta t \ \pi_t \right] \tag{1}$$

1   where, t denotes the current time step, P_t^d is the electricity demand caused by household

2   appliances at time step t, P_t^{PV} is the power generated by the PV system at instant t, Δt is the

3   duration of a simulation time step and π_t is the variable electricity tariff. P_t^{EV+} and P_t^{EV-} are the

4   decision variables and they represent the power charged and discharged by the EV at time

5   instant t, respectively. The above linear energy pricing model reflects the status of the current

6   retail electricity markets, where end-users are price takers and not price makers [26], and is in

7   line with standard optimisation frameworks [26], [28]

8   *Battery degradation cost*

9   As the EV user can be concerned about the underlying battery wear in a charging/discharging

10   process, battery cycling degradation is modelled in this work as a function of three impacting

11   parameters, namely environmental temperature, average SOC and charging/discharging rate.

12   The mathematical model of battery degradation used in this work is empirically developed from

13   laboratory experiments, as obtained from [30]. This model is also in line with leading literature

14   in the topic of lithium-ion battery degradation modelling [31], [32]. The model is described

15   hereby.

$$\underset{P_t^{EV+}, P_t^{EV-}}{argmin} \ \mathcal{F}_2 = \sum_{t=1}^{N^S} \frac{C^B}{2 \frac{0.2}{\alpha_t^c} \bar{E}^{EV} \ DOD} \tag{2}$$

16   where, the numerator, C^B, represents the investment cost of the EV battery and the denominator

17   provides the lifetime energy throughput provided by the battery before it reaches the end of

18   automotive life. It should be noted that the latter depends on the charging/discharging

19   conditions at time step t. In fact, α_t^c is the battery degradation coefficient caused by the

20   decision variables at time step t, $\bar{E}^{EV}$ is the maximum EV battery capacity and DOD is the

21   depth of discharge adopted in the experiments (90%). One cycle is considered in the

22   experiments as an equivalent charging-discharging sequence [hence, the coefficient 2 in

23   Equation (2)]. The battery degradation coefficient models the impact of stress factors on the

24   equivalent lifetime energy throughput and is defined as:

$$\alpha^c = \gamma_1 \left(\gamma_2 T^{b^3} + \gamma_3 T^{b^2} + \gamma_4 T^b + \gamma_5 \right) \times \left(\gamma_6 \langle SOC \rangle + \gamma_7 \right) \times \left(\gamma_8 C_t^r + \gamma_9 \right) \tag{3}$$

where, $\gamma_1, \ldots, \gamma_8$ are fitting parameters, and three stress factors are considered, namely T^{env}, the environmental temperature, $\langle SOC \rangle$, the average SOC in N^s time steps and C_t^r, the charging rate as a percentage of the battery capacity at time step t which can be denoted as below:

$$C_t^r = \frac{P_t^{EV}}{\bar{E}^{EV}} \tag{4}$$

where P_t^{EV} can be either P_t^{EV+} for charging or P_t^{EV-} for discharging, which are assumed to incur the same degradation [29].

Grid net exchange

As households and EVs are connected to the distribution system (DS), to ensure an efficient operation, HMGs must control their power exchange. In fact, the power exchanged by each HMG will impact the DS on a number of levels:

- Excessive power demand leads to higher current circulation, which causes increased network losses [3], [23], [33].
- Electricity peak demand determines the capacity of the network that is required to supply electricity, hence higher demand peaks lead to increased network investments [3], [23], [33], [34].
- Without maximising self-consumption of renewable energy, contingent amount of clean energy will be injected in DSs and without means of consuming it, not only it will be wasted, but it can cause reverse power flows at substations, [33].
- Previous research demonstrated that if the power exchanged with the DS is left uncontrolled, there can be serious voltage instability due to both peak demand and generation excess [3], [23].

It is therefore pivotal to control the power exchanged with the DS, since this preventive measure can minimise and potentially solve such problems [33], [34]. This is done by minimising the net power exchanged with the grid by each HMG as shown in the equation below:

$$\underset{P_t^{EV+}, P_t^{EV-}}{argmin} \ \mathcal{F}_3 = \sum_{t=1}^{N^s} \left| P_t^d - P_t^{PV} + P_t^{EV+} - P_t^{EV-} \right| \Delta t \tag{5}$$

Where the absolute value of the total net exchange is minimised by penalising both high consumption (peak demand) and high generation (excessive PV generation). The same

approaches were adopted in [3] and [33], both of which demonstrated the improvement of the overall network operation when the net energy exchange of each household connected to a DN are minimised, subject to operational constraints (i.e. uncontrollable demand and unconsumed generation). In fact, the resultant voltage profile was maintained persistently closer to the nominal value [3], [33]. Additionally, current peaks, substation loading and reverse power flow were also minimised. Therefore, it can be concluded that if Equation (5) is minimised for every household connected to a DN, compelling benefits in terms of grid stress alleviation can be attained.

It should be noted that the presented objectives are conflicting, i.e. the optimised energy cost, battery degradation, and energy exchange with the network, as expressed in the objective function Equation (1), (2), and (5), respectively, cannot be achieved at the time. In other words, minimising one target may sacrifice the others. To be more specific, to minimise the energy cost, the end electricity user needs to make the most of energy arbitrage following the price signals, which will most likely not match with the charging schedule under net exchange minimisation. This means that the energy cost and the grid net power cannot be optimised simultaneously and approaching the target of either case would however incur increased number of battery cycling, namely higher battery degradation. As such, it can be seen that the conflicts among the three objectives inherently exist, which justifies the need of the MOO strategies proposed in this paper.

The conflict among these three objectives can also be interpreted from the aspect of the mathematical properties of the three objective functions. In fact, these three objective functions in Equations (1), (2) and (5) are formulated as a linear, a quadratic and a nonlinear problem, respectively. The associated optimal solution would naturally lie in different part of the feasible region, and approaching the optimum of one target would sacrifice the others.

2.1.2. Optimisation constraints

A number of constraints must be defined in order to extract from the optimisation process only technically feasible results. Before defining technical constraints, it should be noted that charging and discharging processes will determine the energy stored in the EV battery as defined by the following equation:

$$E_t^{EV} = E_{t-1}^{EV} + \left(\eta^+ P_t^{EV+} - \frac{P_t^{EV-}}{\eta^-} \right) \Delta t \tag{6}$$

1 where, E_t^{EV} is the energy stored in the EV at time step t, η^+ is the efficiency of the charging

2 process, η^- is the discharging efficiency and Δt is the duration of a time step. We assume

3 hereafter, without loss of generality, that the efficiencies of the charging and discharging

4 processes are the same. The key constraints include the maximum power, maximum and

5 minimum energy and desired energy at the departure. The available charging equipment allows

6 the EV to charge and discharge its battery and the exchangeable power is limited by the rating

7 of the hardware. This constraint is described by:

$$0 \leq P_t^{EV+}, P_t^{EV-} \leq \overline{P}^{EV} \tag{7}$$

8 where $\overline{P}^{EV}$ indicates the rating of the charger; here we assume without loss of generality that

9 the maximum charging and discharging ratings are the same.

10 Furthermore, the energy that can be stored in the EV must be limited by its capacity, as

11 expressed by the following equation:

$$\underline{E}^{EV} \leq E_t^{EV} \leq \overline{E}^{EV} \tag{8}$$

12 where $\underline{E}^{EV}$ is the lower energy limit, which has been set to account for unforeseen emergency

13 journeys. One key constraint defined herewith, links the energy states in all the time steps and

14 satisfies the user's travelling requirement:

$$\sum_{t=1}^{N^S} E_t^{EV} \geq (SOC^{dep} - SOC^{arr})\overline{E}^{EV} \tag{9}$$

15 An additional constraint is related to the non-simultaneous charging/discharging process,

16 which can be set follows:

$$P_t^{EV+} \times P_t^{EV-} = 0, \forall t \tag{10}$$

17 It should be noted that the a similar approach as Equation (10) is to use logical variables to

18 control the charging and discharging process [27], however these are not adopted here due to

19 the non-linear objective functions, which would otherwise require complex mixed-integer non-

20 linear solvers.

3. Dynamic programming based multi-objective optimisation algorithm

In this research, a novel multi-objective optimisation algorithm based on dynamic programming (DP) [35] is proposed to balance three objectives, namely end user electricity cost, EV battery degradation and grid stress alleviation.

DP is based on Bellman's principle of optimality [36]. With this approach, the cost function over a time-horizon is divided in sub-cost-functions defined in each time step. This technique exploits the separability property of the objective function, which means that the function can be deconstructed in several objective functions defined for each time step t, which are independent from each other.

This can be suitably applied to EV charging, where the objective functions, Equations (1), (2) and (5), are defined at each time step and a feasible set is defined and dynamically updated based on the constraints, namely Equations (6)-(10). Therefore, with the forward induction approach, as the time-horizon advances, the cost function is calculated for each feasible state at the current time step t and by considering the state of the system at the previous time step. Ultimately, the optimal trajectory is built iteratively by considering the current and the previous time steps, throughout the duration of the simulation.

Upon plugging-in, the initial SOC of the EV is measured (SOC^{arr}) and a desired SOC is set as a target (SOC^{dep}). Let us consider the following mapping of any continuous SOC state at the current time step t, into a discrete set of SOC values: $S_t^q: SOC_t \rightarrow S^q$, where $S^q = [SOC^1, \dots, SOC^q]$. Hence, the SOC at each time step can only assume one among these q values. The arrival and required SOCs are therefore approximated to the nearest discrete counterpart, namely S^A for arrival and S^B for departure. At each time-step t, a set of feasible EV states, satisfying the given constraints, will be considered by the algorithm, defined as X_t^q. Similarly, the set of all feasible root states (states at the previous time step), is X_{t-1}^q. More precisely, let us define the following expressions:

$$W_t^1 = \left\{ S_t^q \in S^q \middle| \frac{\left| SOC_t^i - SOC_{t-1}^j \right|}{\Delta t} \leq \overline{P}^{EV} \right\} \tag{11}$$

and

$$W_t^2 = \left\{ \mathcal{S}_t^q \in S^q \,\middle|\, \mathcal{S}^B - \frac{(N^S - t)\overline{P}^{EV}}{\Delta t} \leq SOC_t^n \leq \mathcal{S}^B + \frac{(N^S - t)\overline{P}^{EV}}{\Delta t} \right\} \tag{12}$$

1 where N^s is the number of time-steps from arrival to departure. Then, let us define the feasible

2 set of EV battery states at time-step t as:

$$X_t^n = \{ \mathcal{S}_t^n \in W_t^1 \cap W_t^2 \subseteq S^n \} \,. \tag{13}$$

3 Once the dynamic (updated at each time step t) feasible set is defined, under DP, at each time

4 step t, the optimal SOC state is chosen in order to minimise the objective function in all the

5 previous and current feasible states, as detailed in the following equation

$$\underset{\mathcal{S}_{t-1,j}^q \in X_{t-1}^q, \mathcal{S}_{t,i}^q \in X_t^q}{\text{argmin}} \mathcal{F}(\mathcal{S}_{t,i}^q) + \mathcal{F}(\mathcal{S}_{t-1,j}^q) \,, \forall i,j \tag{14}$$

6 where $\mathcal{S}_{t,i}^q$ is any i feasible SOC states of the current time step and $\mathcal{S}_{t-1,j}^q$ is any j feasible SOC

7 state in the previous time step.

8 **Remark 1.** The non-linear optimisation problem defined in (1), (2) and (5) with constraints (7-

9 10) are reformulated as the DP approach in (14) with a feasible set defined in (11-13).

10 An evident implication of the above DP reformulation is that the decision variable is the state

11 of the system (EV battery), namely the battery SOC (representative of the energy stored in the

12 battery). However, the two optimisation problems are equivalent (apart from the discretisation)

13 as charging/discharging powers are proportional to the energy stored/discharged for each time

14 step as a consequence of Equation (6), i.e. $E_t^{EV} \propto P_t^{EV+}, P_t^{EV-}$. In fact, the transition between

15 SOC states determines the underlying charging/discharging power according to the equations:

$$\begin{cases} P_t^{EV+} = \frac{\mathcal{S}_t^q - \mathcal{S}_{t-1}^q}{\eta^+} \overline{E}^{EV} \\ P_t^{EV-} = 0 \end{cases} \,, if \; \mathcal{S}_t^q - \mathcal{S}_{t-1}^q \geq 0 \tag{15a}$$

$$\begin{cases} P_t^{EV+} = 0 \\ P_t^{EV-} = \eta^- \left(\mathcal{S}_t^q - \mathcal{S}_{t-1}^q \right) \overline{E}^{EV} \end{cases} \,, if \; \mathcal{S}_t^q - \mathcal{S}_{t-1}^q < 0 \,. \tag{15b}$$

16 Alongside, the constraints defined in Equations (7-10) have been suitably reformulated with

17 the definition of a dynamic feasible set in Equations (11)-(13). Equation (15) and (11)

18 reformulate Equations (6), (7) and (10). Equation (12) verifies the constraints related to energy

19 bounds and satisfaction of charging requirements, namely Equations (8) and (9). Figure 3

provides a graphical explanation of the above concept. As time progresses, the feasible step is updated based on the rating of the charger, energy bounds, target energy and the number of time steps to the next departure. When the next departure time comes, i.e. $t = N^s$, the feasible set only contains one possible state, $S_{N^s}^q = S^B$.
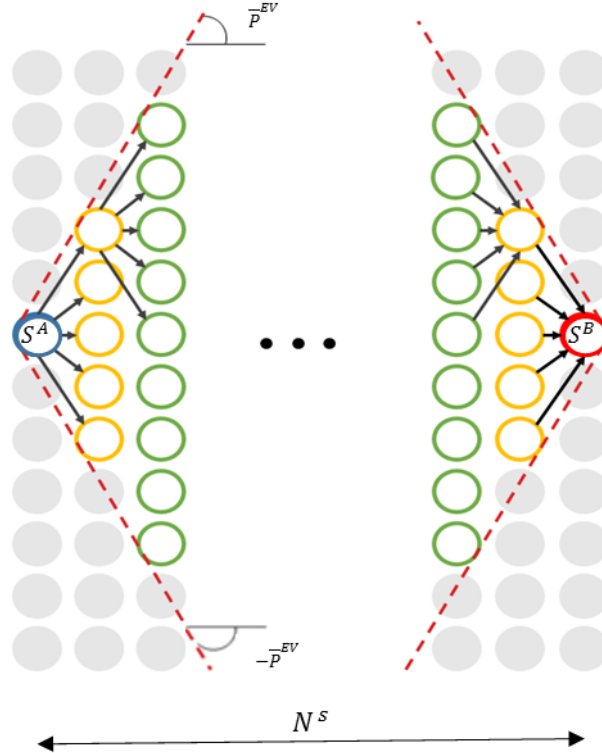
Figure 3. Illustration of SOC states and feasible set

As the basic DP strategy has intrinsic shortcomings, which we discuss herewith, we further adapted this approach to suit a multi-objective formulation. The traditional DP explores the full search space by comparing every possible combination of states, from the beginning state to the final state. This is a nearly exhaustive search and is notably demanding in computation effort. As in MOO a Pareto front must be found, which may contain several optimal solutions at each time-step, a pure DP approach would exacerbate the computational time required to evaluate all possible Pareto options. To overcome this obstacle, we propose some improvements to the basic DP approach. It is worth pointing out that an effective solution to real-time MOO based on DP is yet to be proposed in literature. In fact, the methods proposed in literature are deterministic and cannot deal with the uncertain nature of many systems in real-life (as it is the case for PV generation) [37], [38]. In this work, we propose an online multi-objective dynamic programming (OMODP) approach, which makes use of predictions of PV generation and electricity demand to schedule EV charging in real-time with a model predictive control (MPC) approach [39]. Some basic definitions for MOO can be found in [40].

1 The proposed optimisation problem can be characterised as follows:

Predictive optimisation problem
  Non-linear program with N^s continuous variables
  Objective functions: Equations (1), (2) and (5)
  Constraints: $2N^s$ bound constraints in Equation (7), N^s linear constraints in
  Equation (8), 1 linear constraint in Equation (9) and N^s non-linear constraints
  in Equation (10)
Dynamic programming
  Optimisation algorithm n discrete variables
  Objective function: Equation (14)
  Definition of feasible set with Equations (11)-(13)

---

2 When dealing with a MOO problem is essential to determine all the non-dominated solutions,

3 which are the set of solutions that are not better or worse than other solutions. This is because,

4 due to the conflict among objectives, if one charging/discharging schedule performs well along

5 one objective, it may not achieve a good score along another objective. The most

6 straightforward way for obtaining non-dominated solutions is to check that all the solutions

7 found by the optimisation algorithm are not mutually dominating, with a process known as

8 Non-dominated sorting [40]. Without specifying any priority rules for the objectives, the full

9 Pareto front is the set of optimal solutions. A range of preference based methods can be used

10 to identify the optimal solution aligned with the stakeholders' priorities, including a-priori

11 methods [41] and interactive methods [42]. In this work, an a-priori method, Analytical

12 Hierarchy Process (AHP), was used to make decisions of the optimal solution. When applying

13 the AHP technique, a final score is assigned based on the available options and the priorities

14 of the decision-makers and this score will determine which solution to choose from the Pareto

15 front. More technical details on AHP can be found in [41]. The pair-wise comparison matrices

16 (element i, j represents the priority of objective i over objective j; if the element is 1 it means

17 that the objectives are equally important, if it is higher than one, objective i has higher priority

18 than objective j, whereas if is lower than one then objective j has more importance than

19 objective i) for the three prioritisation rules, namely, energy cost, battery degradation cost and

20 grid net exchange are shown in Table 2.

21 Table 2 Pairwise comparison matrix under three prioritisation rules

	Priority on electricity cost				Priority on battery degradation				Priority on grid net exchange		
	Obj_1	Obj_2	Obj_3		Obj_1	Obj_2	Obj_3		Obj_1	Obj_2	Obj_3
Obj_1	1	5	9	Obj_1	1	5	2	Obj_1	1	$\frac{1}{2}$	$\frac{1}{9}$

| Obj_2 | $\frac{1}{5}$ | 1 | 2 | Obj_2 | $\frac{1}{5}$ | 1 | 9 | Obj_2 | 2 | 1 | $\frac{1}{5}$ |
| Obj_3 | $\frac{1}{9}$ | $\frac{1}{2}$ | 1 | Obj_3 | $\frac{1}{2}$ | $\frac{1}{9}$ | 1 | Obj_3 | 9 | 5 | 1 |

1 It should be pointed out that the prioritisation rules set in this work have been decided based

2 on the natural tendency of the three key stakeholders, as described in Section 2.1. The proposed

3 approach allows any other consistent priority rule to be set; for instance, the results from a

4 survey, as the one in [43] can be utilised to formulate the weights. In practice, these rules can

5 be derived from surveys or set by contractual terms between the stakeholders. For example, the

6 DSO can agree with the EV user a prioritisation rule that values grid net exchange in return of

7 a revenue stream. This can allow the DSO to defer grid investments as the demand peak will

8 be reduced, achieving a win-win situation for both stakeholders.

9 The pseudo-code of OMODP is provided hereby.

OMODP algorithm

Input: predictions $P_2^{PV}, \dots, P_{N^s}^{PV}, P_2^{d}, \dots, P_{N^s}^{d}$, measurements for each time step P_t^{PV}, $P_t^{d}, \overline{E}^{EV}, \underline{E}^{EV}, \overline{P}^{EV}$ SOC^{in}, t^{dep}, SOC^{dep}, objectives $\mathcal{F}_1, \dots, \mathcal{F}_m$ and user priorities $\beta^1, \dots, \beta^m$

Return: current set point for the charger I_t^{EV} for each time step t

1: **for** $t \leftarrow 1$ **to** (N^s) **do**

2: **Initialisation:** MPC optimisation $\begin{cases} \text{argmin}(\mathcal{F}_1) \\ \quad \vdots \\ \text{argmin}(\mathcal{F}_m) \end{cases}$ to determine $\sigma_t = [S_t^1, \dots, S_t^m]$, the energy status under each objective.

3: Define feasible SOC range, X_t^q from Equation (13) and map $\sigma_t \rightarrow \sigma_t^q$ (discrete states). Update feasible set as $\chi_t^n = X_t^q \cap \sigma_t^q$

4: **if** $t = 1$

5: Compute $\begin{cases} \mathcal{F}_1(S^A, S_t^n) \\ \quad \vdots \\ \mathcal{F}^m(S^A, S_t^n) \end{cases}$, $\forall S_t^n \in \chi_t^n$

6: **else**

7: Compute $\begin{cases} \mathcal{F}_1(S_{t-1}^{op}, S_t^n) \\ \quad \vdots \\ \mathcal{F}_m(S_{t-1}^{op}, S_t^n) \end{cases}$, $\forall S_t^n \in \chi_t^n$

8: **end if**

9: Apply non-dominated sorting to determine the Pareto frontier at t, $\mathbf{P}_t^n$

10: Apply AHP with $\beta^1, \dots, \beta^m$ to choose $\{S_{t-1}^*, S_t^*\}$. Store S_t^* as S_t^{op}.

11: Determine charging/discharging power from Equation (15)

12: Measure battery voltage $V_{t meas}^b$

13: Calculate current set-point $I_t^{b*} = \dfrac{P_t^{EV}}{V_{t meas}^{EV}}$

14:	Update $SOC^{in} = SOC_{t^{meas}}$ with Coulomb counting by measuring battery current $I^b_{t^{meas}}$
15:	**end for**

The algorithm requires predictions for the future PV generation and electricity demand, current measurements of PV generation and demand, the objectives to be optimised as well as the requirements for the next departure and priorities of the objectives from the user. In accordance with the next departure, the number of optimisation time-steps is defined, and initial predictive optimisations are carried out with MPC (step 2, in the pseudo-code). Under this approach, the generation and demand measurements along with predictions over the time horizon are used to determine three SOC set points. The maximum and minimum of these set points constitute the boundaries to constrain the DP method (step 3). Once the feasible region has been defined with MPC, DP is implemented to calculate the values of the different objectives in correspondence to all the SOC states in the feasible region, for the current and next time step (steps 4-8). Subsequently, Pareto efficient solutions are found by performing Non-dominated sorting [40] (step 9). It should be noted that the Pareto frontier will be different for each time step as the system status changes in time (the energy stored in the battery changes, the remaining scheduling time decreases etc.), hence at each time step a different Pareto frontier will be computed, namely $\mathbf{P}^n_t$. AHP is implemented to choose a global optimal solution in line with the user priorities (step 10); the chosen optimal SOC status is stored in memory (S^{op}_t). The associated charging/discharging power is calculated from Equation (16) (step 11). Finally, an optimal current set point is communicated to the bidirectional charger by dividing the power value by the measured battery voltage for the measurement time step t^m (steps 12-13). The current SOC of the EV is updated with the Coulomb counting technique (step 14), as also implemented in [8]. The algorithm has been implemented for real-time control of EV charging, under three cases, representing three different priority choices as be presented in the appendix.

3.1. Prediction of system variables

For the implementation of OMODP a number of system variables need to be predicted, namely, household electricity demand and PV generation profile. In this work, a combination of K-means clustering [44], and regression tree has been used to predict future household electricity demands, while the PV generation has been predicted using and artificial neural network (ANN).

1 Flowcharts detailing the electricity demand prediction process can be found in Figure A. 1 and

2 Figure A. 2 in the Appendix. The result of the electricity demand clustering process is shown

3 in Figure A. 3. ANNs aim at emulating the processes of a biological brain, with connections

4 (edges) linking one artificial neuron to another. Artificial neurons, grouped in layers, receive

5 inputs which are summed and passed to other neurons after applying a non-linear function.

6 There are weights associated to the neurons and edges, which decide the strength of the

7 connection and are adjusted during the learning process. Interested readers are directed to [45]

8 for further insights. In this research an ANN with two layers, one hidden and one output layer,

9 with 12 and 19 neurons, respectively, and both with a Hyperbolic tangent sigmoid transfer

10 function has been used to predict the daily PV generation profile. The input data for the ANN

11 is presented in Table A. 1 and the training performance is shown in Figure A. 4 of the

12 Appendix. The R value for the training, validation and test phase of the ANN model was 0.967,

13 0.9555 and 0.936, respectively, indicating good prediction capability. It should be noted that

14 in the present work, the uncertainty of stochastic variables, i.e. household electricity demand

15 and PV generation, is captured using prediction strategies, as in [10], [13], [16], [18], [21],

16 [22], and other methods are also available in literature such as stochastic optimisation [11],

17 [12], robust optimisation [20], [46], and ensemble prediction-based strategies [47], which

18 manage to reduce the impact of prediction errors.

19 4. Case study setting

20 In order to validate the effectiveness of the OMODP algorithm developed in the present work,

21 a number of case studies ranging have been implemented. Table 3 lists all the presented cases

22 along with the prioritisation rules set by users and simulation setup.

23 Table 3. Details of the case studies

Case study	Prioritised objective	Type	Time horizon	Travelling pattern
Case 1	Energy cost	Simulation	Two days	Randomly generated
Case 2	Bat. deg. cost			from probability
Case 3	Grid net exchange			distributions obtained
Case 4	Energy cost	Comparison with ANEC		from the UK National Travel Survey [48]

24 The first three cases aim at showing the effectiveness of the OMODP algorithm in pursuing

25 three objectives at the same time and make real-time decision based on the set priorities. The

26 fourth case serves as a comparison between OMODP and the established ANEC algorithm.

27 The last three cases show the multi-objective real-time charge control of a commercial 18650

1 battery in a laboratory experiment. A GUI was developed as an interactive tool (refer to Figure

2 A. 5 of the Appendix) where users can set their travelling requirements and receive information

3 on the status of the EV and the local electricity system, i.e. household electricity demand and

4 PV generation.

5 Figure 4 shows the real electricity demand and PV generation profiles, compared with the

6 predictions obtained with the methods developed in Section 3.1, as well as the wholesale

7 electricity price, used for case studies 1-4. PV generation has been represented as negative

8 power consumption to ensure clarity. It can be seen that the prediction algorithm is effective in

9 anticipating the variation of demand and generation. However, the peak levels are not well

10 predicted. This is due to the dependence of the electricity consumption at a domestic scale on

11 the habits of the inhabitants. This, however, does not constitute a major obstacle as real-time

12 measurements are fed to the optimisation algorithm along with the forecasts in order to decide

13 the charging/discharging level. Furthermore, as the demand peaks last only for limited time,

14 for instance due to the activation of a household device, the algorithm can correct its decision

15 from the real-time measurement.
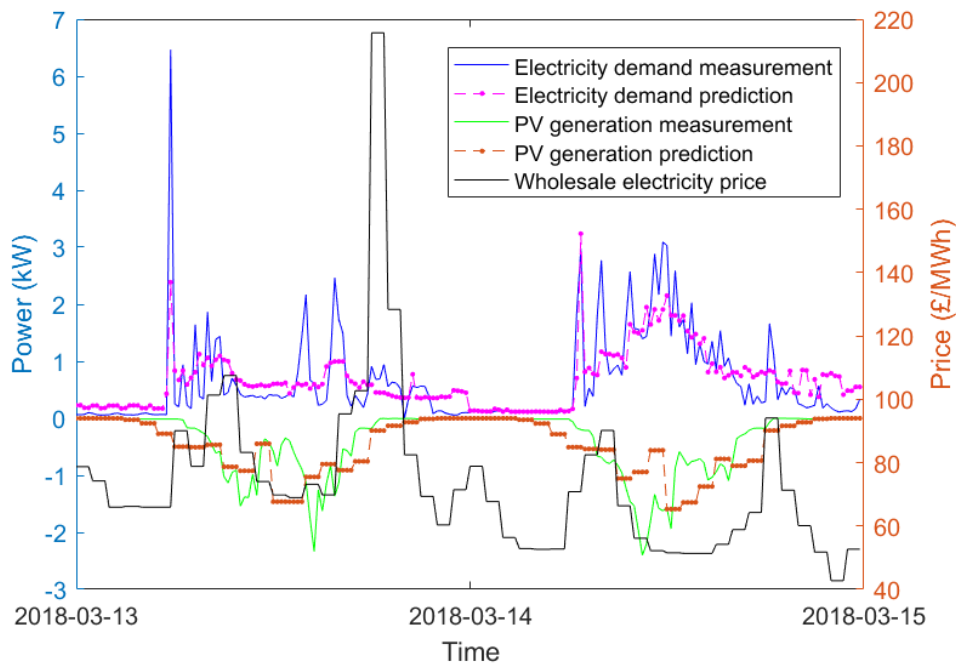
16

17 Figure 4. Real and predicted profiles for electricity demand, generation (left axis) and electricity price (right

18 axis)

19 The simulated travelling requirements for the four case studies are shown in Table 4.

Table 4. EV travelling requirements for cases 1-4

Parameters	Case 1	Case 2	Case 3	Case 4
Arrival time (yyyy-mm-dd HH:MM)		12:45		
Departure time (yyyy-mm-dd HH:MM)		07:30		
Energy at arrival (kWh)	12	12	12	25
Desired energy at departure (kWh)		25		

2 The optimisation algorithm has been implemented in Matlab 2018a using the fmincon solver,

3 which utilises an interior point algorithm with a barrier function. More details can be found in

4 [49].

5. Simulation results

6 Figure 5 depicts the charging/discharging schedule issued by the OMODP algorithm for cases

7 1-3 and Table 5 shows the associated performance for the three objectives. It can be seen from

8 Figure 6 that in all the three cases, charging/discharging events are initiated only when the EV

9 is available at home, in agreement with the specifications provided in Table 4. Furthermore,

10 when the EV is charged to minimise the energy cost of the HMG, the EV power exchange

11 profile follows the wholesale electricity price profile: during the evening price spike, the EV

12 discharges at full rate and recharges back in the morning, prior to departure, when the price is

13 lower. The results of this arbitrage are quite evident in Table 5, where under case 1, the energy

14 cost is the lowest when compared with other cases. This approach can be effortlessly adopted

15 to any other price signal, i.e. fixed tariffs, time-of-use tariffs etc.

16
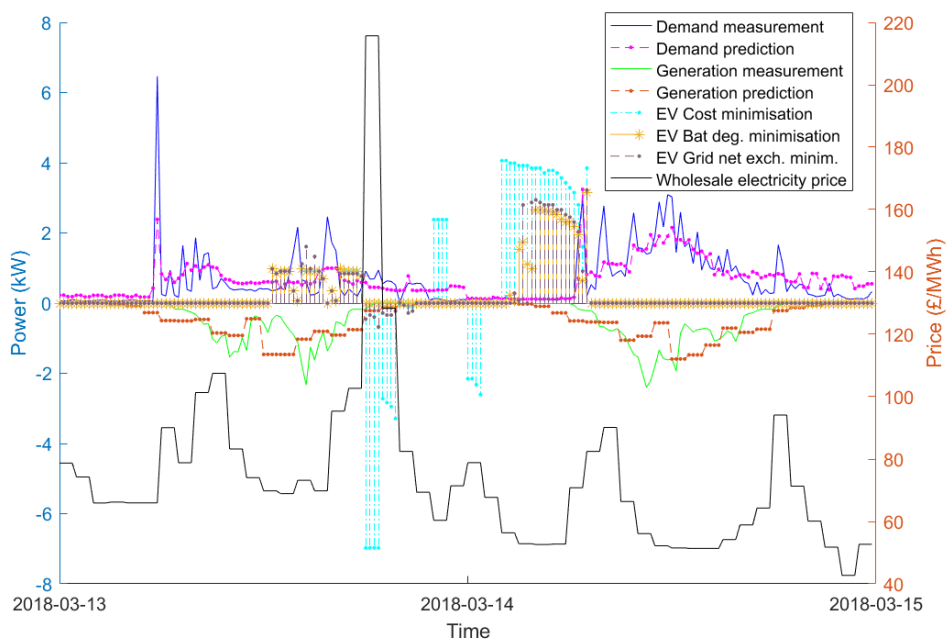
1   Figure 5. Charging/discharging profiles (left axis) and electrcity price (right axis) for cases 1-3

2   Table 5. Achieved performance along the three objectives for cases 1-3

Case study	$\mathcal{F}_1$ (£)	$\mathcal{F}_2$ (£)	$\mathcal{F}_3$ (kWh)
Case 1	0.42	0.1213	3.62
Case 2	1.79	0.0697	2.77
Case 3	1.69	0.0772	2.74

3   When battery degradation minimisation is prioritised (Case 2), the charging rate is overall

4   lower than all the other cases (compare brown continuous stems with blue dashed stems) to

5   minimise the adverse impact of high charging rates. In addition, no discharging events are

6   initiated; this is due the degradation caused by the discharging process which would not make

7   up the saving in degradation caused by low average SOC. As both degradation terms are

8   multiplied together in Equation 5, it is their combination that increases degradation. For the

9   same reason, not all charging is carried out just before departure but also upon arrival; in fact,

10   this would cause a higher degradation due to the higher charging rate. On the other hand, when

11   grid net exchange minimisation was the main priority, the EV is used to provide the few

12   demand spikes (during the price peak and later in the evening of 13-03-2018). Furthermore,

13   notice the difference between the charging schedule under case 3 during the only demand peak

14   in the morning, just prior to departure. While under the other cases the EV is charged to reach

15   the desired SOC, charging under case 3 is slowed down to reduce the adverse impact of the

16   electricity demand peak on the DN. In fact, under Case 3, the EV is charged more before and

17   after that demand peak.

18   Figure 5 and Table 5 showed that the OMODP algorithm is able to adapt in real-time to the

19   preference shown by the decision maker, which highlights its MOO properties.

20   Figure 6 and Table 6 present the results for case 4, where the OMODP algorithm has been

21   tested against an established method, like ANEC.
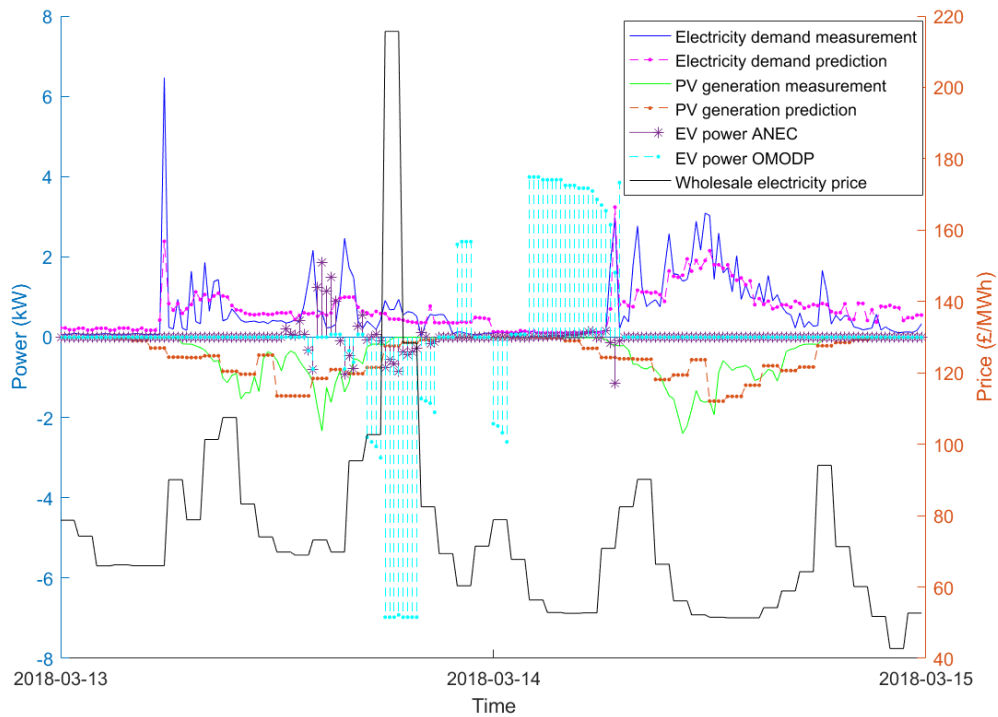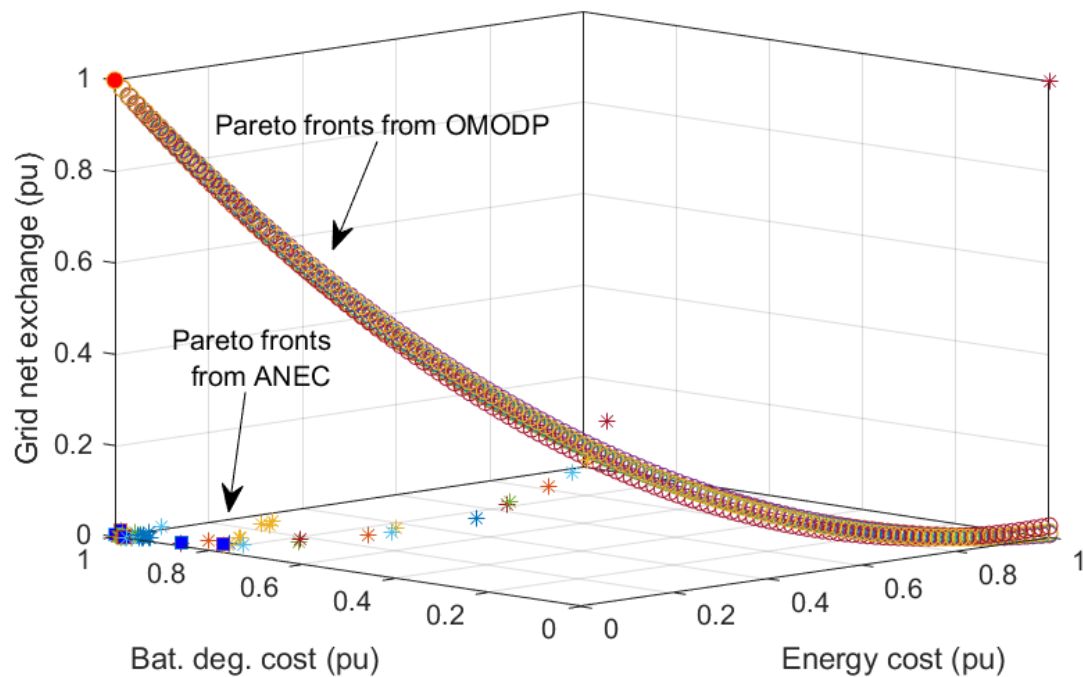
Figure 6. Comparison between OMODP and ANEC power profiles (left axis) and electricity price (right axis) for case 4

Table 6. Comparison between OMODP and ANEC's performance along three objectives for case 4

Case study 4			
Algorithm	$\mathcal{F}_1$ (£)	$\mathcal{F}_2$ (£)	$\mathcal{F}_3$ (kWh)
ANEC	0.80	0.041	2.05
OMODP	-0.88	0.195	3.80

It is evident from Figure 6 and Table 6 that the OMODP algorithm is more effective than ANEC in achieving the a lower energy cost (it should be noted that a negative energy cost indicates a revenue), in line with the prioritisation set in Table 2 and Table 3. In fact, OMODP is able to bring a revenue to the HMG owner. This comes at the expense of a higher battery degradation cost, which however is offset by the incurred revenues. It should also be pointed out that this was expected as the main priority was energy cost minimisation and a prioritisation rule that values battery degradation more can be easily set (see case 2).

The ability of OMODP of achieving a lower energy cost lies in its capability of better exploring the search space than ANEC, as evidenced by Figure 7.

Figure 7. Comparison between the normalised dynamic Pareto fronts achieved with OMODP (Pareto optimal solutions are scatters and red dots are the chosen solution) and ANEC (Pareto optimal solutions are the asterisks and blue squares are the chosen solutions) for 6 arbitrary time steps.

When assessing the quality of the Pareto frontiers, the major advantage of OMODP lies quite evidently in the diversity and regularity of the Pareto optimal solutions, which on the other hand is not achieved by ANEC frontiers. It can be seen that Pareto frontiers attained with ANEC are fragmented, irregular and concentrated around a subset of the full search space. On the other hand, OMODP stroke a better balance between exploration and exploitation. In fact, the frontiers with OMODP are better distributed throughout the entire search space, exploring also extremal solutions. For example, it can be seen from Table 6, that when pursuing the minimum energy cost, OMODP provides a solution that was not covered by ANEC (energy cost in ANEC was double of that with OMODP). OMODP would therefore allow more flexibility to the decision maker who would be able to make a more informed decision than with ANEC.

Perhaps an even more compelling advantage of OMODP can be seen in Figure 8, where OMODP overwhelmingly outperformed ANEC in terms of computational time. In fact, in the beginning ANEC can take even more than 150 seconds to compute the Pareto front, while OMODP would always take less than 5 s. This was due to the inherent computational burden brought by the augmented ε-constraint algorithm implemented in ANEC, which exhibits a

quadratic growth as the desired granularity of the Pareto frontier increases. OMODP on the other hand computes a more diverse Pareto front in a fraction of the time, because of the much simpler and more effective heuristic used in evaluating the three objectives for regular SOC steps. The performance exhibited by OMODP is comparable with the fast methods presented in [8] and [15], but with a higher degree of detail in the optimisation due to the multi-objective calculation. It should be pointed out that with lower computational time, OMODP is better positioned than methods like ANEC in flexibility markets that require fast response, while still offering multi-objective capabilities.
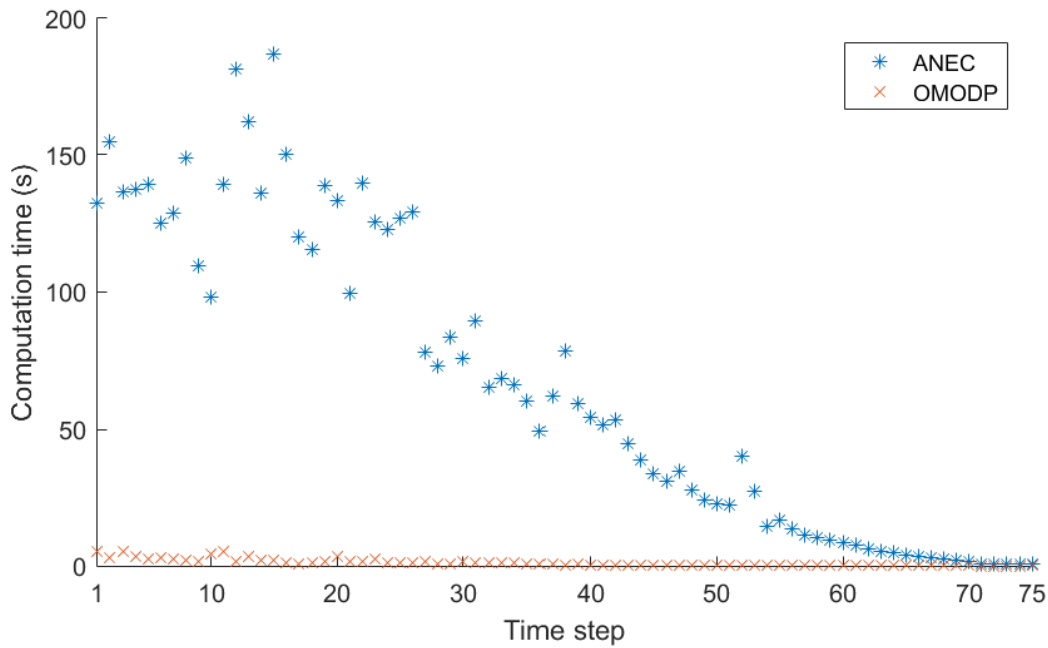
Figure 8 Comparison between the computational time of OMODP versus ANEC

6. Experimental demonstration

To demonstrate the effectiveness of the proposed charge control algorithms, a number of experiments, designated as cases a-c, were performed in a laboratory setup without any commercial electric vehicles. A commercial 18650 battery storage cells were used, which will be designated as EV hereafter. Table 7 provides the specifications for the experimental demonstration.

Table 7 Specifications of the experimental demonstration cases

Case	Prioritised objective	Type	Time horizon	Travelling pattern
Case a	$\mathcal{F}_1$		One day	

Case b	$\mathcal{F}_2$	Experimental	Arrival, departure times
Case c	$\mathcal{F}_3$	demonstration	and energy required
			randomly chosen

1   A functional diagram describing the experimental setup and the information flow is presented

2   in Figure 9.
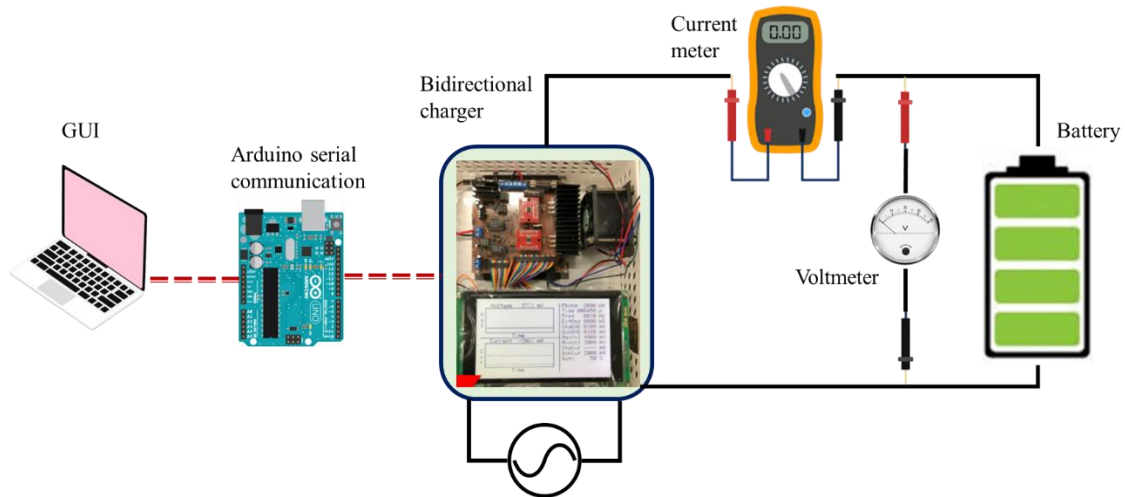
Figure 9 Schematic of the experiment for real-time optimisation

5   The experimental setup contains several hardware and software that together emulate an

6   HMG as depicted in Figure 1 . An Arduino UNO board is used to communicate (red dashed

7   connection in Figure 9) the optimal charging schedule to the battery charger, which then

8   implements the charging/discharging command. Table A. 2 in the Appendix provides a

9   summary of the main specifications of the components in the experiment setup. Voltage

10   and current measurements (dashed lines) are taken to capture the battery's status and sent

11   to the MATLAB code (wide communication bus). The OMODP algorithm is run in

12   MATLAB and the optimal schedule is communicated to the Arduino board, which transfers

13   it to the charger. Although the charger is bidirectional, it is not regenerative, which means

14   that the discharged energy is not sent back to the grid but dissipated in the form of heat.

15   For this reason, the objective in this section is to emulate a MG as often a real MG has a

16   higher rating and is grid-connected. This was only a hardware and regulatory limitation, as

17   in the UK, the market of bidirectional chargers is notoriously immature [50], and additional

18   standards need to be followed to enable grid injection. These limitations, however, do not

19   influence the validity of the proposed management algorithm which can be tested with the

20   available hardware. Nevertheless, the proposed algorithm can be easily coupled with a

21   bidirectional regenerative charger, in a MG at any rating, which would then implement real

22   V2G. Two current probes have been used to measure positive and negative currents as they

1 only capture currents in the positive direction. The travelling pattern emulated for cases a-
2 c is presented in Table 8. As the real-time operation was tested, the experiments were run
3 primarily during office hours, therefore the time period did not match that of commuters
4 (as were the simulated case 1-4).

5 Table 8. Travelling pattern for cases a-c

Parameters	Case a	Case b	Case c
Objective priorities		From Table 2	
Available time (yyyy-mm-dd HH:MM)	2019-12-15 15:15	2019-12-16 10:35	2019-12-14 13:00
Departure time (yyyy-mm-dd HH:MM)	2019-12-15 21:15	2019-12-16 16:45	2019-12-14 19:00
Desired capacity at departure (Ah)	1.7	2.2	2.4

6

7 It can be seen from Table 8, that the battery was made available for the different experimental
8 cases according to the associated available and departure time. The OMODP algorithm
9 generated one Pareto frontier for each time slot of 15 minutes in that time period, and then
10 chose the optimal solution each time step according to the set priorities. Figure 10 to Figure 15
11 depict the charging schedules and associated Pareto frontiers for the three case studies. In the
12 first case, i.e. minimising energy cost, it could be seen that the battery is charged in
13 correspondence of the minimum prices, in the availability window (6 hours, from 3 to 9) and
14 during the period with high-energy price, no charging is initiated. However, it can be seen that
15 the final capacity fell short of 0.1 Ah; this was due to both inefficiencies in the charging
16 equipment (round-trip losses were higher than expected) and the strict availability period,
17 which meant that the EV left almost as soon as the price spike terminated, not leaving the
18 algorithm enough time to catch the final schedule. Also by looking at the Pareto frontiers in
19 Figure 11, it could be seen that there was an overall agreement among the three objectives as
20 in most of the time steps, the frontiers were only points. This indicates that there was not much
21 room left for other decisions; only one charging schedule was feasible.

22 By observing the charging current in Figure 12, it can be seen that in order to minimise the
23 average SOC, the battery is kept uncharged for as long as possible, with charging being initiated
24 only after 2:30 pm. Looking at the Pareto frontiers in Figure 13, it could be seen that in
25 accordance with the priorities specified, only the solutions characterised with the minimum
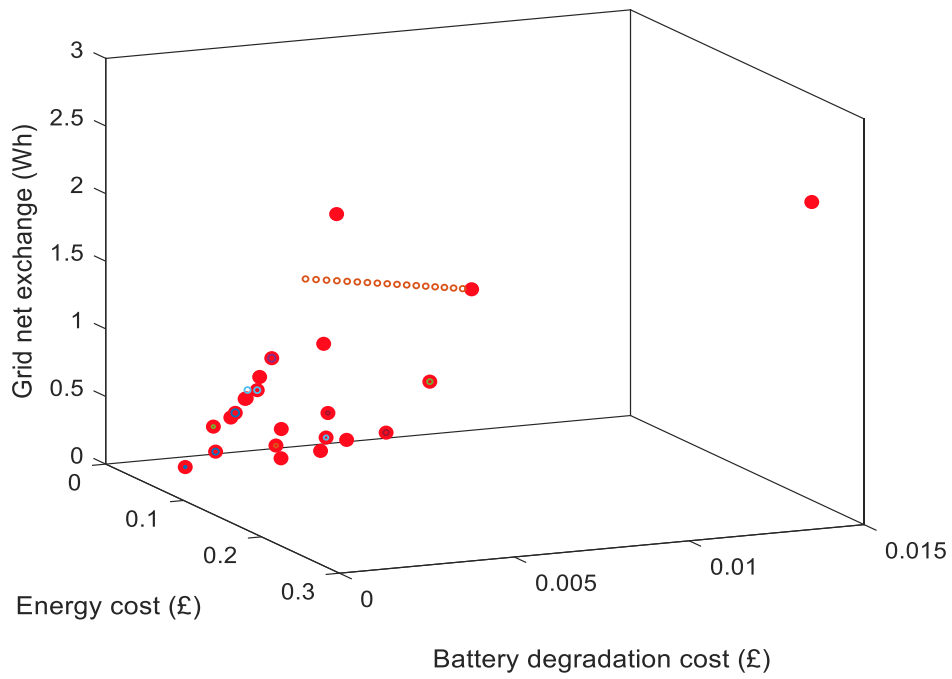
1   battery degradation (leaning towards the farthest left) have been issued in the form of charging

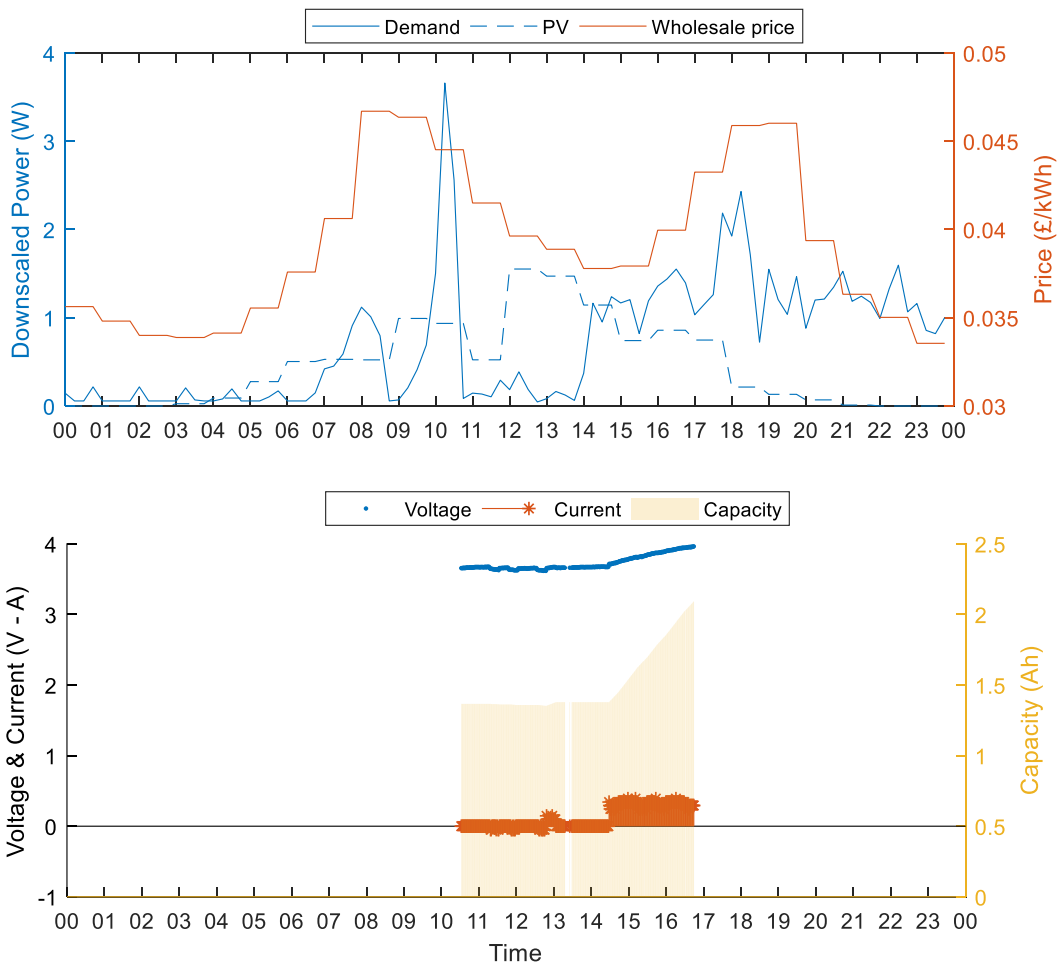2   schedules.
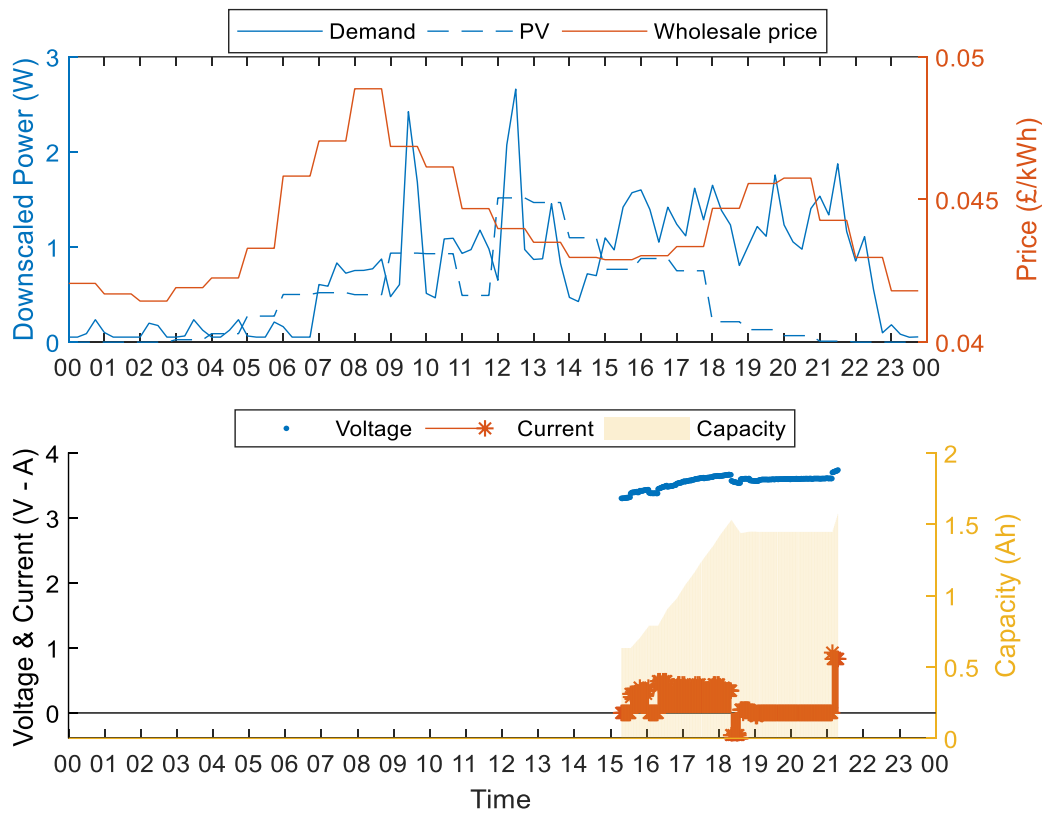
3

4   Figure 10. Real-time charging profile for case study 1
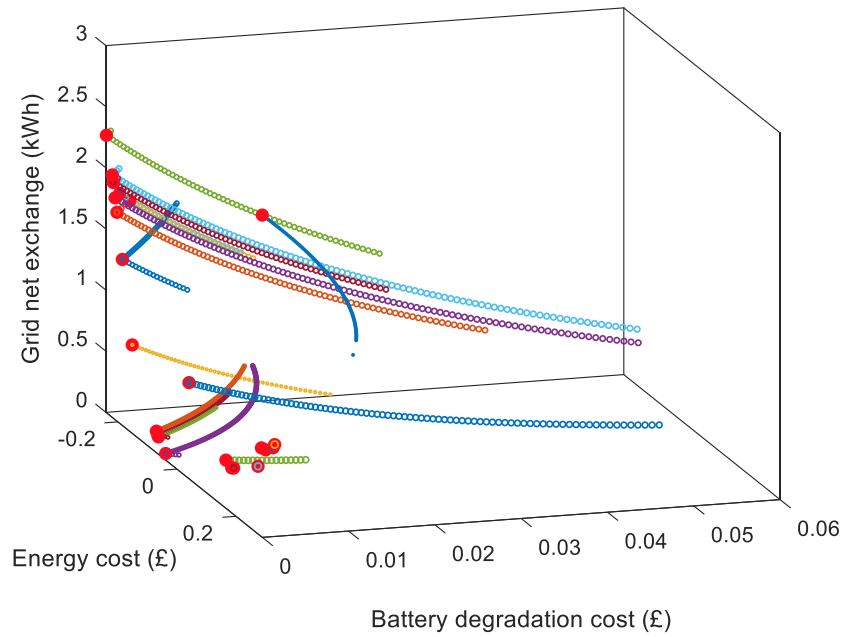
1

2   Figure 11. Pareto frontiers (scatters) and chosen solutions (red dots) in case study a
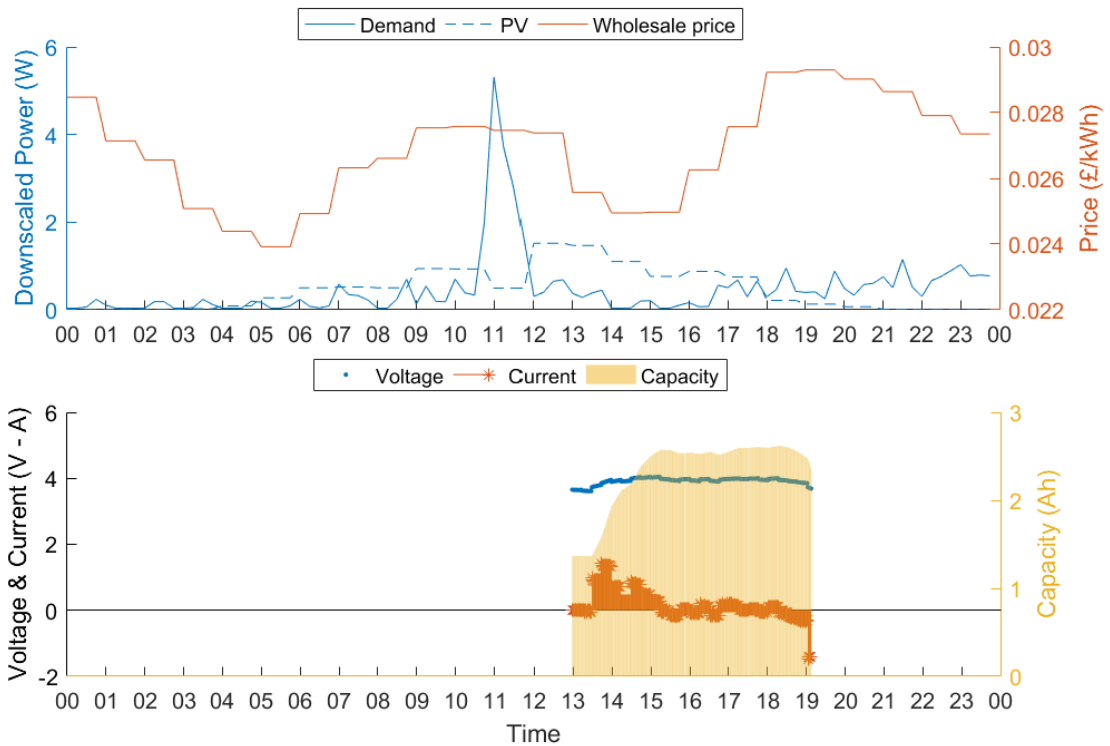

3

1   Figure 12. Real-time charging profile for case study b

2

3   Figure 13. Pareto frontiers (scatters) and chosen solutions (red dots) in case study b

4

5   Figure 14. Real-time charging profile for case study c

6   As can be seen from Figure 14, EV charging is scheduled between 13:00 to 19:00 hrs in

7   accordance with the availability specified by the user. At 13:30 hrs there is availability of

8   excess PV generation, since the electricity demand is low, hence the EV is charged, while

following the PV generation profile. Charging power is reduced after 3 as the battery exceeds the capacity requested by the user (2.44 Ah). After that moment, the battery is subject to shallow charge and discharge cycles, while following the shape of the electricity demand. After 18:00 hrs the electricity demand is higher than the available PV energy (which is almost negligible). Therefore. the battery is discharged to provide the demand making use of the additional energy that was charged when PV energy was abundant. Overall, the battery was made available for 6 hours, which corresponds to 24 steps of 15 minutes each. OMODP generated a Pareto frontier for each of these time steps, which are shown in Figure 15 along with the chosen solutions (red dots).
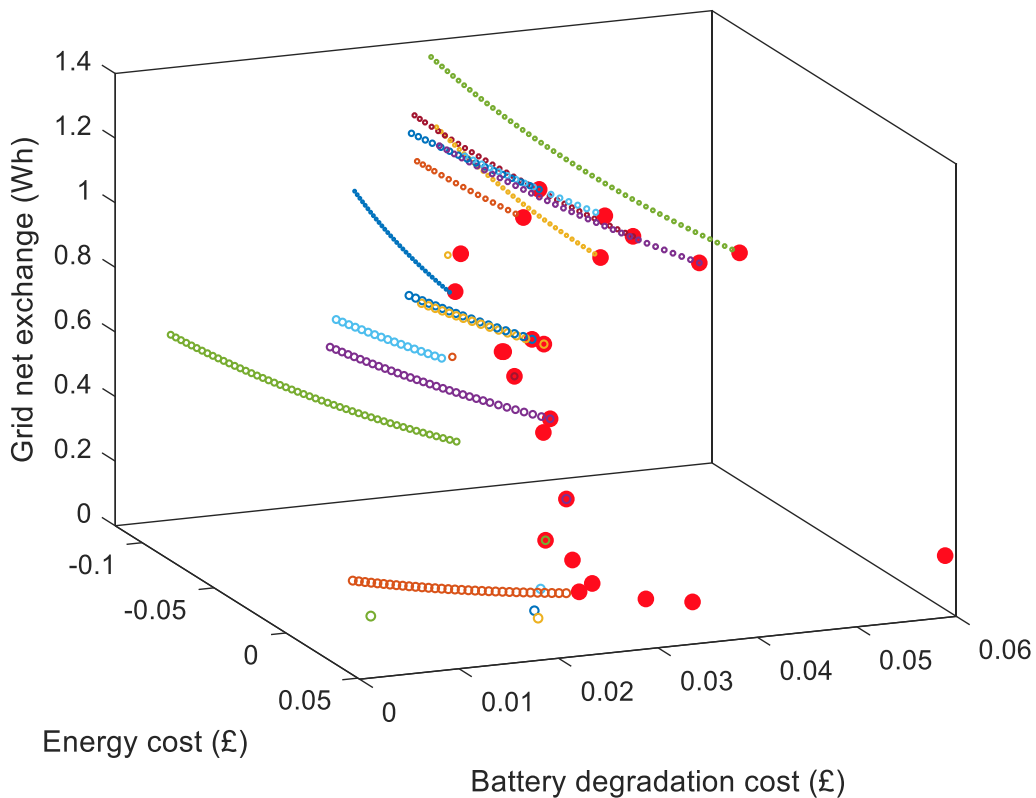
Figure 15. Pareto frontiers (scatters) and chosen solutions (red dots) in case study c

It can be seen that OMODP always choses the solution that gives the lowest grid net exchange (as low as possible along the z axis), in accordance with the priorities set in Table 2. In addition, it can be noticed that the Pareto frontiers do not contain the same number of efficient solutions. This is because, the predictive optimisations (see the OMODP algorithm in Section 3) and the constraint on requested energy limit the SOC swing allowed by the algorithm (the final steps have only few Pareto members because the algorithm is reaching the required SOC target).

7. Conclusions

In this paper a real-time multi-objective optimisation strategy was applied to EV charging and discharging. A demonstration of the energy management agent, the OMODP algorithm, was provided. This optimisation system applies to home-micro-grids, equipped with a photovoltaic system and an EV. The objectives attained by OMODP are electricity cost reduction, battery degradation minimisation and grid net power exchange minimisation. A dynamic programming based multi-objective optimisation method was proposed and applied to seven case studies. The OMODP algorithm did not only outperform a previously developed multi-objective optimisation algorithm but it also exhibited superior computational performance. In fact, the benefits under OMODP were twofold compared to the ANEC method and the computational time was constantly kept below 5s; in comparison, ANEC required at times as much as 180s to issue one charging schedule. This trait is important for real-time applications, where less time dedicated to computation translates to better performance in markets that require fast response. The OMODP algorithm was then applied to three experimental tests in a small-scale setup, while prioritising the three objectives and the measurements showed optimal charging patterns. As the algorithm considers the interests of several stakeholders, it brings together key parties involved in the operation of smart grids and promotes an efficient and sustainable utilisation from clean energy sources. The impact of the proposed optimisation methodology for a cluster of households can provide additional insights on the attainable system level benefits, and this constitute a future investigation topic.

Acknowledgements

References

[1] International Energy Agency, "Global EV Outlook 2020 – Entering the decade of electric drive?", 2020. [Online] Available: https://www.iea.org/reports/global-ev-outlook-2020 [Accessed: Jun. 19, 2020].

[2] National Grid ESO, "Future Energy Scenarios", July 2019. [Online] Available: http://fes.nationalgrid.com/media/1409/fes-2019.pdf. [Accessed: Jun. 19, 2020].

[3] M. Nicoli, R. Das, Y. Wang, G. Putrus, R. Turri and R. Kotter, "A Smart Grid Modelling Tool for Evaluating Optimal Control of Electric Vehicles," *2018 53rd International Universities Power Engineering Conference (UPEC)*, Glasgow, 2018, pp. 1-6. doi: 10.1109/UPEC.2018.8541956.

[4] R. Gough, C. Dickerson, P. Rowley and C. Walsh, 'Vehicle-to-grid feasibility: A techno-economic analysis of EV-based energy storage', in *Applied Energy*, Vol. 192, pp 12-23, January 2017.

[5] J. Liu and C. Zhong, "An economic evaluation of the coordination between electric vehicle storage and distributed renewable energy", in *Energy*, vol. 186, 2019.

[6] U. Datta, N. Saiprasad, A. Kalam, J. Shi and A. Zayegh, "A price-regulated electric vehicle charge-discharge strategy for G2V, V2H, and V2G", in *International Journal of Energy Research*, vol. 43, pp. 1032-1042, 2019.

[7] G. Platt, "The decentralised control of electricity networks intelligent and self-healing systems", 2007.

[8] G. F. Savari, V. Krishnasamy, J. Sathik, Z. M. Ali and S. H.E. A. Aleem, "Internet of Things based real-time electric vehicle load forecasting and charging station recommendation", in *ISA Transactions*, vol. 97, pp. 431-447, 2020.

[9] T. Zhang, H. Pota, C-C Chu, and R. Gadh, "Real-time renewable energy incentive system for electric vehicles using prioritization and cryptocurrency", in *Applied Energy*, vol. 226, pp. 582-594, 2018.

[10] W. Jiang and Y. Zhen, "A Real-Time EV Charging Scheduling for Parking Lots With PV System and Energy Store System," in *IEEE Access*, vol. 7, pp. 86184-86193, 2019, doi: 10.1109/ACCESS.2019.2925559.

[11] Z. Liu, Q. Wu, M. Shahidehpour, C. Li, S. Huang and W. Wei, "Transactive Real-Time Electric Vehicle Charging Management for Commercial Buildings With PV On-Site Generation", in *IEEE Transactions on Smart Grid*, vol. 10, no. 5, pp. 4939-4950, Sept. 2019. doi: 10.1109/TSG.2018.2871171

[12] Z. Liu, Q. Wu, K. Ma, M. Shahidehpour, Y. Xue and S. Huang, "Two-Stage Optimal Scheduling of Electric Vehicle Charging Based on Transactive Control," in *IEEE Transactions on Smart Grid*, vol. 10, no. 3, pp. 2948-2958, May 2019. doi: 10.1109/TSG.2018.2815593.

[13] R. Wang, P. Wang and G. Xiao, "Two-Stage Mechanism for Massive Electric Vehicle Charging Involving Renewable Energy," in *IEEE Transactions on Vehicular Technology*, vol. 65, no. 6, pp. 4159-4171, June 2016. doi: 10.1109/TVT.2016.2523256.
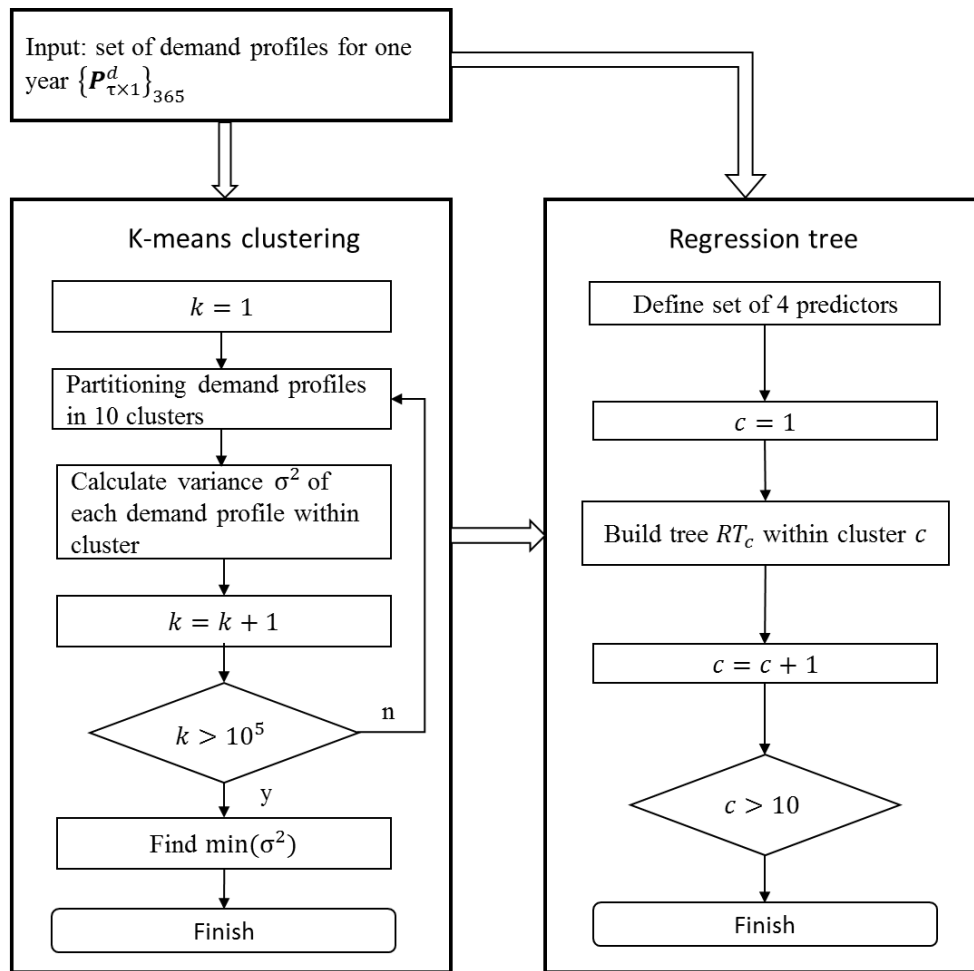
[14]   L. Yao, W. H. Lim and T. S. Tsai, "A Real-Time Charging Scheme for Demand Response in Electric Vehicle Parking Station," in *IEEE Transactions on Smart Grid*, vol. 8, no. 1, pp. 52-62, Jan. 2017. doi: 10.1109/TSG.2016.2582749.

[15]   S. Singh, V. B. Pamshetti and S. P. Singh, "Time Horizon-Based Model Predictive Volt/VAR Optimization for Smart Grid Enabled CVR in the Presence of Electric Vehicle Charging Loads," in *IEEE Transactions on Industry Applications*, vol. 55, no. 6, pp. 5502-5513, Nov.-Dec. 2019. doi: 10.1109/TIA.2019.2928490.

[16]   Y. Hu, S. Su, L. He, X. Wu, T. Ma, Z. Liu and X. Wei, "A Real-Time Multilevel Energy Management Strategy for Electric Vehicle Charging in a Smart Electric Energy Distribution System". Energy Technol., 7: 1800705. 2019. doi:10.1002/ente.201800705.

[17]   Y. Luo, G. Feng, S. Wan, S. Zhang, V. Li and W. Kong, "Charging scheduling strategy for different electric vehicles with optimization for convenience of drivers, performance and transport system and distribution network", in *Energy*, vol. 194: 116807, 2020.

[18]   C. Deng, N. Liang, J. Tan, and G. Wang, "Multi-Objective Scheduling of Electric Vehicles in Smart Distribution Network," *Sustainability*, vol. 8, no. 12, p. 1234, Nov. 2016.

[19]   R. J. Hamidi and H. Livani, "Myopic real-time decentralized charging management of plug-in hybrid electric vehicles", in *Electric Power Systems Research*, vol. 143, pp. 522-532, 2017.

[20]   M. Latifi, A. Khalili, A. Rastegarnia and S. Sanei, "A Bayesian Real-Time Electric Vehicle Charging Strategy for Mitigating Renewable Energy Fluctuations," in *IEEE Transactions on Industrial Informatics*, vol. 15, no. 5, pp. 2555-2568, May 2019. doi: 10.1109/TII.2018.2866267.

[21]   Y. Xiong, B. Khakit, C. Chu and R. Gadh, "Real-Time Bi-Directional Electric Vehicle Charging Control with Distribution Grid Implementation," *2018 IEEE/PES Transmission and Distribution Conference and Exposition (T&D)*, Denver, CO, 2018, pp. 1-5. doi: 10.1109/TDC.2018.8440426.

[22]   F. Grée, V. Laznikova, B. Kim, G. Garcia, T. Kigezi, and B. Gao, "Cloud-Based Big Data Platform for Vehicle-to-Grid (V2G)," *World Electric Vehicle Journal*, vol. 11, no. 2, p. 30, Mar. 2020.

[23]   G. A. Putrus, P. Suwanapingkarl, D. Johnston, E. C. Bentley and M. Narayana, "Impact of electric vehicles on power distribution networks," *2009 IEEE Vehicle Power and Propulsion Conference*, Dearborn, MI, 2009, pp. 827-831. doi: 10.1109/VPPC.2009.5289760.

[24]   R. Das, Y. Wang, G. Putrus, R. Kotter, M. Marzband, B. Herteleer and J. Warmerdam, "Multi-objective techno-economic-environmental optimisation of electric vehicle for energy services", in *Applied Energy*, vol. 257: 113965, 2020.

[25]   https://www.ovoenergy.com/electric-cars/vehicle-to-grid-charger

[26]   A. Mohsenian-Rad, V. W. S. Wong, J. Jatskevich and R. Schober, "Optimal and autonomous incentive-based energy consumption scheduling algorithm for smart grid," 2010 Innovative Smart Grid Technologies (ISGT), Gothenburg, 2010, pp. 1-6, doi: 10.1109/ISGT.2010.5434752.

[27]   R. Carli, M. Dotoli, J. Jantzen, M. Kristensen and S. B. Othman, "Energy scheduling of a smart microgrid with shared photovoltaic panels and storage: The case of the Ballen marina in Samsø", Energy, vol. 198, 117188, 2020.

[28]   S. M. Hosseini, R. Carli and M. Dotoli, "Robust Optimal Energy Management of a Residential Microgrid Under Uncertainties on Demand and Renewable Power Generation," in IEEE Transactions on Automation Science and Engineering, doi: 10.1109/TASE.2020.2986269.

[29]   S. Saxena, Y. Xing, D. Kwon, M. Pecht, "Accelerated degradation model for C-rate loading of lithium-ion batteries", in *International Journal of Electrical Power & Energy Systems*, vol. 107, pp. 438-445, 2019.

[30]   Das, Ridoy (2020) Multi-objective Smart Charge Control of Electric Vehicles. Doctoral thesis, Northumbria University.

[31]   K. Uddin, T. Jackson, W. D. Widanage, G. Chouchelamane, P. A. Jennings, J. Marco, "On the possibility of extending the lifetime of lithium-ion batteries through optimal V2G facilitated by an integrated vehicle and smart-grid system", Energy, Vol. 133, pp. 710-722, 2017.

[32]   M. Dubarry, A. Devie and K. McKenzie, "Durability and reliability of electric vehicle batteries under electric utility grid operations: Bidirectional charging impact analysis", Journal of Power Sources, vol. 358, pp. 39-49, 2017.

[33]   A. Paladin, R. Das, Y. Wang, Z. Ali, R. Kotter, G. Putrus and R. Turri, "Micro Market based Optimisation Framework for Decentralised Management of Distributed Flexibility Assets", Renewable Energy, vol. 163, pp. 1595-1611, 2020.

[34]   R. Hemmati and H. Mehrjerdi, "Investment deferral by optimal utilizing vehicle to grid in solar powered active distribution networks", Journal of Energy Storage, vol. 30, pp.101512, 2020.

[35] D. Huang, Y. Gu, H. Wang, Z. Liu, and J. Chen, "An Incentive Dynamic Programming Method for the Optimization of Scholarship Assignment," in *Discrete Dynamics in Nature and Society*, 2018.

[36] R. Bellman, "The Theory of Dynamic Programming", in *Bulletin of the American Mathematical Society*, vol 60, pp. 503-515, 1954.

[37] T. Zhao and J. Zhao, "Improved multiple-objective dynamic programming model for reservoir operation optimization", in *Journal of Hydroinformatics*, vol. 16, 2014.

[38] J. Mahmoudimehr and P. Sebghati, "A novel multi-objective Dynamic Programming optimization method: Performance management of a solar thermal power plant as a case study", in *Energy*, vol. 168, pp. 796-814, 2019.

[39] M. Nikolaou, "Model predictive controllers: A critical synthesis of theory and industrial needs", in *Advances in Chemical Engineering*, Academic Press, vol. 26, pp. 131-204, 2001.

[40] K. Deb, S. Agrawal, A. Pratap and T. Meyarivan, "A Fast Elitist Non-dominated Sorting Genetic Algorithm for Multi-objective Optimization: NSGA-II". in Schoenauer M. et al. (eds) Parallel Problem Solving from Nature PPSN VI. PPSN 2000. Lecture Notes in Computer Science, vol 1917. Springer, Berlin, Heidelberg.

[41] R.W. Saaty, "The analytic hierarchy process—what it is and how it is used", in *Mathematical Modelling*, vol. 9, pp. 161-176, 1987.

[42] Y. -N. Guo, X. Zhang, D. -W. Gong, Z. Zhang and J. -J. Yang, "Novel Interactive Preference-Based Multiobjective Evolutionary Optimization for Bolt Supporting Networks," in IEEE Transactions on Evolutionary Computation, vol. 24, no. 4, pp. 750-764, Aug. 2020, doi: 10.1109/TEVC.2019.2951217.

[43] J. Geske and D. Schumann, "Willing to participate in vehicle-to-grid (V2G)? Why not!", in *Energy Policy*, vol. 120, pp. 392-401, 2018.

[44] A. Likas, N. Vlassis and J. J. Verbeek, "The global k-means clustering algorithm", in *Pattern Recognition*, vol. 36, pp. 451-461, 2003.

[45] J. A. Anderson, "An Introduction to Neural Networks", MIT Press, 1995.

[46] J. S. Giraldo, J. A. Castrillon, J. C. López, M. J. Rider and C. A. Castro, "Microgrids Energy Management Using Robust Convex Programming," in IEEE Transactions on Smart Grid, vol. 10, no. 4, pp. 4520-4530, July 2019, doi: 10.1109/TSG.2018.2863049.

[47] Y. Guo, H. Yang, M. Chen, J. Cheng and D. Gong, "Ensemble prediction-based dynamic robust multi-objective optimization methods", Swarm and Evolutionary Computation, vol. 48, pp. 156-171, 2019. https://doi.org/10.1016/j.swevo.2019.03.015

1   [48]   https://www.gov.uk/government/collections/national-travel-survey-statistics

2   [49]   https://uk.mathworks.com/help/optim/ug/constrained-nonlinear-optimization-

3   algorithms.html#bsgppl4

4   [50]   V2G Global Roadtrip: Around the world in 50 projects, UK Power Networks, Technical

5   report, October 2018. Available online at: https://innovation.ukpowernetworks.co.uk/wp-

6   content/uploads/2018/12/V2G-Global-Roadtrip-Around-the-World-in-50-Projects.pdf

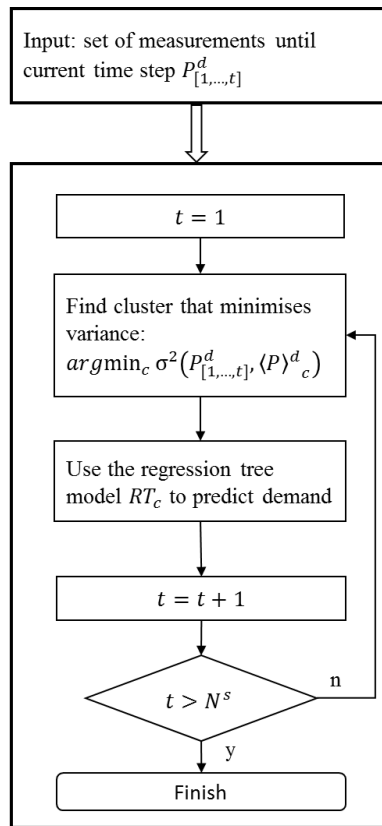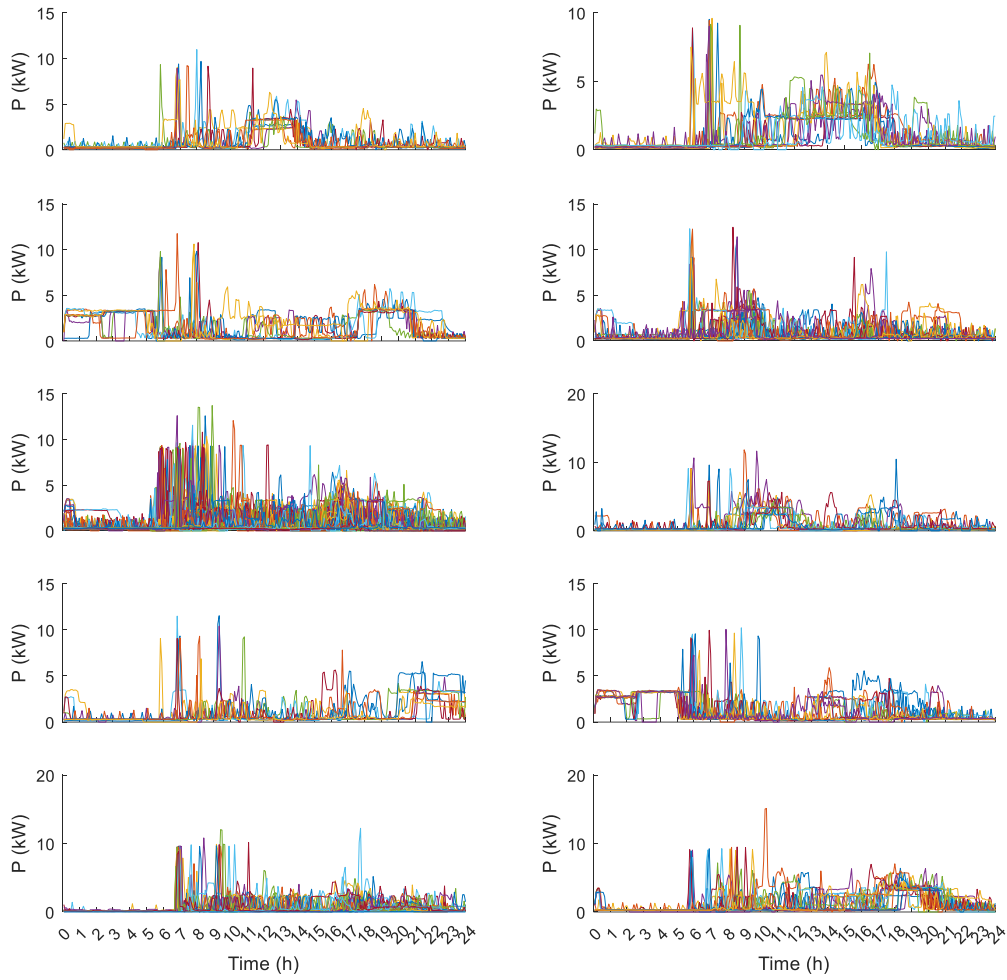7   [51]   https://solcast.com/

1 **Appendix**

Figure A. 1 Flow-chart implemented for building the demand predictor

2

3

Input: set of measurements until current time step $P^d_{[1,...,t]}$

$t = 1$

Find cluster that minimises variance:
$arg\min_c \sigma^2\left(P^d_{[1,...,t]}, \langle P \rangle^d_c\right)$

Use the regression tree model RT_c to predict demand

$t = t + 1$

$t > N^s$

n

y

Finish

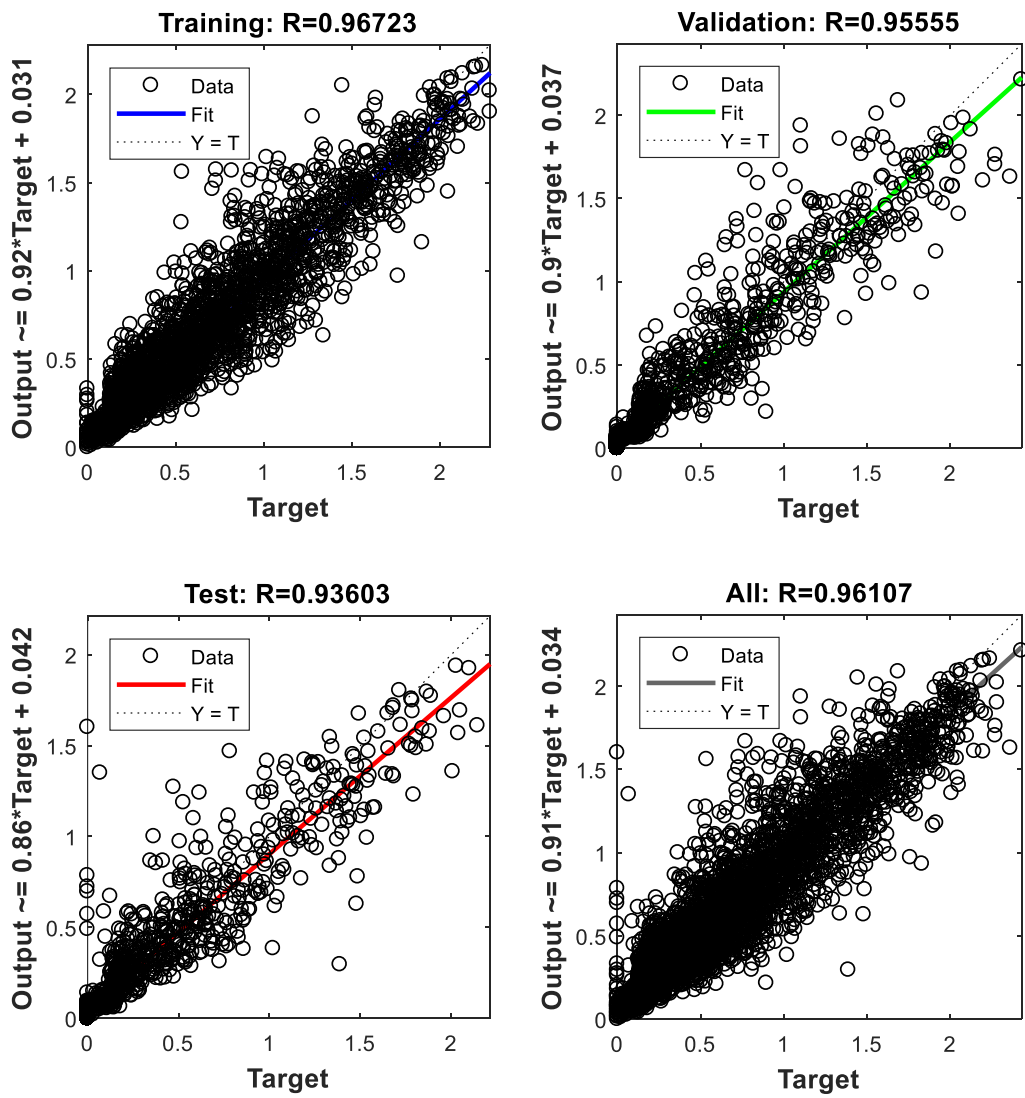Figure A. 2 Flowchart for real-time demand prediction

1

2

3

Figure A. 3 Household electricity demand profiles for one year clustered in 10 clusters

Table A. 1 Input data for ANN training

Parameter	Resolution
Global horizontal irradiation	Hourly
Air temperature	Hourly
Function indicating the seasonal effect $f^{seas} = \sin\left(d \times \frac{2\pi}{365} - \frac{\pi}{2}\right) + 1$	Single value

Training: R=0.96723

Validation: R=0.95555
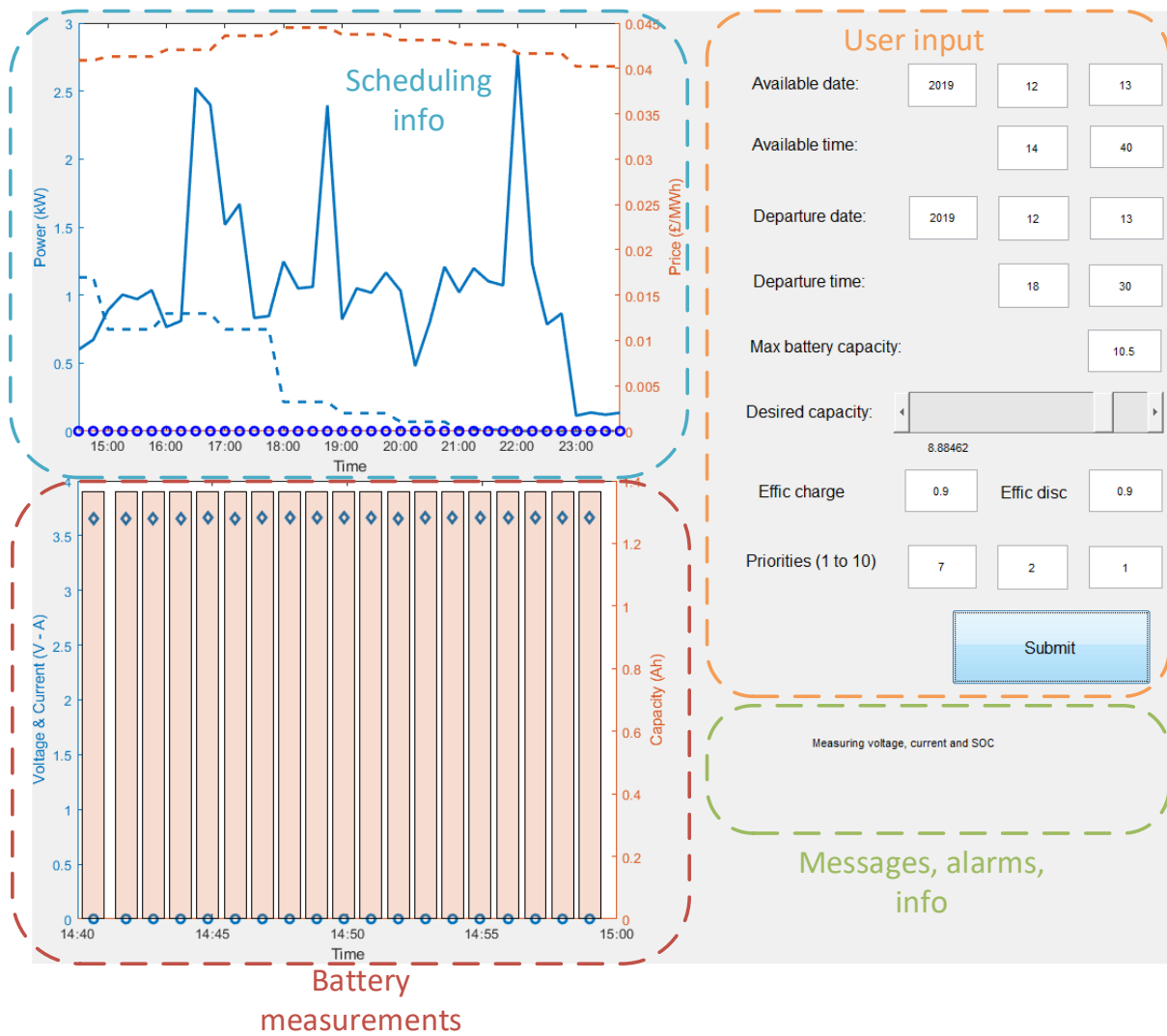
Test: R=0.93603

All: R=0.96107

1

2   Figure A. 4 Training performance of an ANN for PV generation prediction

Figure A. 5 Developed GUI for interactive setting of multi-objective optimisation based EV charging

Table A. 2 Main specifications of the HMG components

Photovoltaic system	
Simulated 4 kWp; weather data retrieved from [51]	
Battery system	
Parameter	**Value**
Technology	Lithium-Ion
Capacity	3.2 Ah
Internal resistance	60 mΩ
Maximum voltage	4.2 V
Minimum voltage	3 V
Battery charger	
Parameter	**Value**
Maximum power	27 W
Maximum voltage	9 V
Maximum current	3 A
Measurements	Voltage, current

Desktop computer	
Parameter	**Value**
Processor	AMD PRO A4-350B R5 3500MHz
RAM	8 GB
Software	MATLAB 2018a
Communication	Serial
Simulation time step t	15 min
Arduino Uno R3	
Analog measurements	A_0 voltage, A_1 charging current, A_5 discharging current and D_5 control signal
Measurement time step t^m	1 min
Measurements	
Current measurements	2xAgilent N2774A current probes

1

2

3